Benchmark Study on Neutronics Performance of Liquid Blankets

Li, Zaixin

Doctor of Philosophy

Department of Fusion Science
School of Physical Sciences
The Graduate University for Advanced Studies

2007

CONTENTS

ABSTRACT

Self-cooled Li and Flibe blankets with V-alloy structure are attractive concepts and considered for the LHD-type helical fusion reactor design FFHR. Maximum thickness allowed for blanket is 1.2 m in FFHR. Blanket functions such as heat removal due to 14 MeV D-T fusion neutrons, breeding of tritium fuel and radiation shielding must be fulfilled within this thickness.

To verify blanket functions, detailed neutronics investigations are required. One of the key options for Li and Flibe blankets is the use of neutron multiplier Be because, in spite of potential benefit of Be from neutronics aspects, there are some issues specific to Be such as irradiation effects. Thus it is necessary to evaluate quantitatively the impact of Be on tritium breeding ratio (TBR), radiation shielding and radio activation. For Li blanket, it is necessary to apply an electrical insulating coating e.g. Er_2O_3, to reduce the magneto-hydro dynamic (MHD) pressure drop when Li flows in a strong magnetic field. However, neutronics investigation on the effect of Er_2O_3 is scarce.

To provide the reactor design with viable data, the neutronics analysis procedure including transport and activation codes and nuclear libraries applied to liquid blankets need to be examined and, if necessary, improved. For this purpose, benchmark studies with systematic comparison of calculations and experiments are necessary.

The objectives of the present study are:

To investigate Li and Flibe blankets for FFHR by neutronics analysis with focus on the effect of Be and Er2O3 coating on TBR, shielding and activation.

To examine or improve the neutronics calculation procedure for application to liquid blankets by comparison with activation experiments using D-T neutrons.

In the neutronics assessment of FFHR, 3 dimension Monte Carlo code MCNP-4C with JENDL3.2 pointwise nuclear data file and FISPACT-2001

code with EAF-2001 file in 175 energy groups were used for neutron transport and activation calculations, respectively. The results obtained are qualitatively assumed as follows: Use of Be can significantly improve TBR for both Li/V-alloy and Flibe/V-alloy blankets. For the Li/V-alloy blanket with Be, the shielding property can be greatly improved maintaining the adequate TBR. On the other hand, the shielding property of the Flibe/V-alloy blankets with and without external Be is comparable. The quantitative estimate of the effects of Er_2O_3 coating showed that the activation of the coating could influence the long-term activation property of the structural components. However, recycle of materials for the structural components is still feasible with Er_2O_3 coating in 10 μm thickness. With 1μm thickness of the coating, the activation level of the blanket is close to the hands-on recycling limit.

For the purpose of verifying or improving the neutronics calculation procedure, especially activation analysis of liquid blankets, a series of irradiation experiments were performed using Fusion Neutronics Source (FNS) at Japan Atomic Energy Agency (JAEA), which is well-suited to neutronics study relevant to a D-T fueled reactor. The specimens of V-4Cr-4Ti, Er and Teflon in 10 mm×10 mm×0.03-0.1 mm were prepared for studying the activation of V-alloy structure, MHD coating of Er_2O_3, and F in molten salt Flibe, respectively. In addition to the assembly for direct D-T neutron irradiation, Be, Li and Li/Be mock-ups were assembled to examine the dependence of the activation on neutron spectrum expected in fusion blankets.

The activities of specimens measured with a high purity Ge detector were compared with the calculations using FISPACT-2001 codes and EAF-2001 file. The neutron flux calculated by MCNP-4C was used as input file in FISPACT-2001 calculation. In this study, the continuous-energy cross-section data were also used in activation calculation in the limited cases in addition to the data of EAF-2001 in 175 and 315 energy groups.

Comparison of calculation (175 groups) to experiment (C/E) shows that

the values of C/E for most of radioactive nuclides (^{18}F, ^{48}Sc, ^{161}Er, etc) produced by reactions with high-energy threshold lie in the range of 0.8-1.2. A significant underestimation for ^{168}Ho (C/E 0.62) was found in D-T neutron irradiation case. It could be caused by the effects of coarse energy grouping near 14 MeV because ^{168}Er(n,p)^{168}Ho has a threshold energy close to 14 MeV and its cross-section rises steeply around 14 MeV. In fact, the C/E value of ^{168}Ho calculated with continuous-energy cross-section approached unity.

The comparisons of activation for ^{171}Er and ^{52}V, both of which are the products of (n, γ) reactions, were performed with activation data in 175, 315 energy groups and continuous data. For ^{52}V, the major contribution is the reaction with thermal neutrons. Using 315 group cross sections, C/E values of ^{52}V show a clear trend approaching to unity relative to those using 175 energy groups case because of the finer group structures in thermal neutrons range. The results also agree well with the results using the continuous-energy cross section. The reaction ^{170}Er(n, γ)^{171}Er has a huge resonance peak at 95 keV. Large overestimations for ^{171}Er were observed with group data due to the coarse grouping in the resonance region. Use of continuous-energy cross-section provided much better agreement with experiment for Be mock-up, where the neutron flux is almost constant with energy in the resonance range. On the other hand, for the case of Be/Li mock-up, where the flux rapidly increases with energy in the resonance range, large discrepancy (C/E ~ 1.17) was observed even with continuous cross-section. This result clearly indicates the necessity for re-evaluation of the cross-section data of ^{170}Er(n, γ)^{171}Er reaction. This issue was disclosed through the comparative examination of C/E in various neutron spectra, and thus unique achievement of this study.

Conclusions of the present study are:

A) Detailed neutronics characterization of Li and Flibe blankets using V-alloy structure for FFHR has, for the first time, been carried out:

A-1) Advantage of the use of Be is quantified. With Be, TBR design margin

for Li and Flibe blankes could be improved. For Li blanket with Be, the shielding design margin could also be improved with adequate TBR. The results provide information necessary for characterizing trade-off of using Be in Li and Flibe blankets.

A-2) The Er_2O_3 coating induces the long-term radioactivity of Li blanket. However, recycle of structural materials is still feasible with Er_2O_3 coating in 10 μm thickness. Thinner Er_2O_3 coating is necessary for realizing hands-on recycling.

B) Experimental studies of activation characteristics for materials in Li and Flibe blankets have been carried out using a D-T neutron source, especially for the first time for the Er_2O_3 coating:

B-1) For the threshold reactions, where the threshold energy is close 14 MeV and its cross-section rises steeply around 14 MeV, continuous-energy cross-section data is needed.

B-2) For the (n, γ) reaction with high cross-section at thermal neutrons region, finer grouping is necessary.

B-3) Use of continuous-energy cross-section is necessary for (n, γ) reaction with dominant resonance peak in medium energy ranges.

B-4) The cross section data of $^{170}Er(n, \gamma)^{171}Er$ needs re-evaluation.

CHAPTER 1

Introduction

1.1 Fusion energy

1.1.1 World energy demand and supply

Figure 1.1 shows the world primary energy sources in use in 2000 [1]. About 80% energy consumption is from fossil fuels. Burning fossil fuels to obtain energy causes air pollution, acid rain and production of CO_2. The release of CO_2 causes a critical environmental issue of "green house effect", which induces global warming and may cause more critical issues of abominable global climate change.

Fossil fuels are not renewable energy resource. It was predicted based on present energy consumption rates that oil, natural gas and coal will be used up within 20-70 years, 30-70 years and several hundred years, respectively [2]. On the contrary, the energy demand increases with the growth of population and enhanced industrialization/living standards. R. Toschi [3] concluded that present renewable energy sources may not be able to meet the increasing energy demand in long term. Figure 1.2 shows the trend of energy consumption in unit of billion barrels of oil equivalent per year (bb/y) [4]. It can be seen that energy shortfall will occur in less than 50 years and be enhanced gradually with time. Mankind must therefore develop new energy options to solve the near-term and long-term demand of energy. Fusion energy is one of the proposed options [5-9]. Fusion power offers the potential of a relatively clean, safe and almost limitless source of energy [10-12].

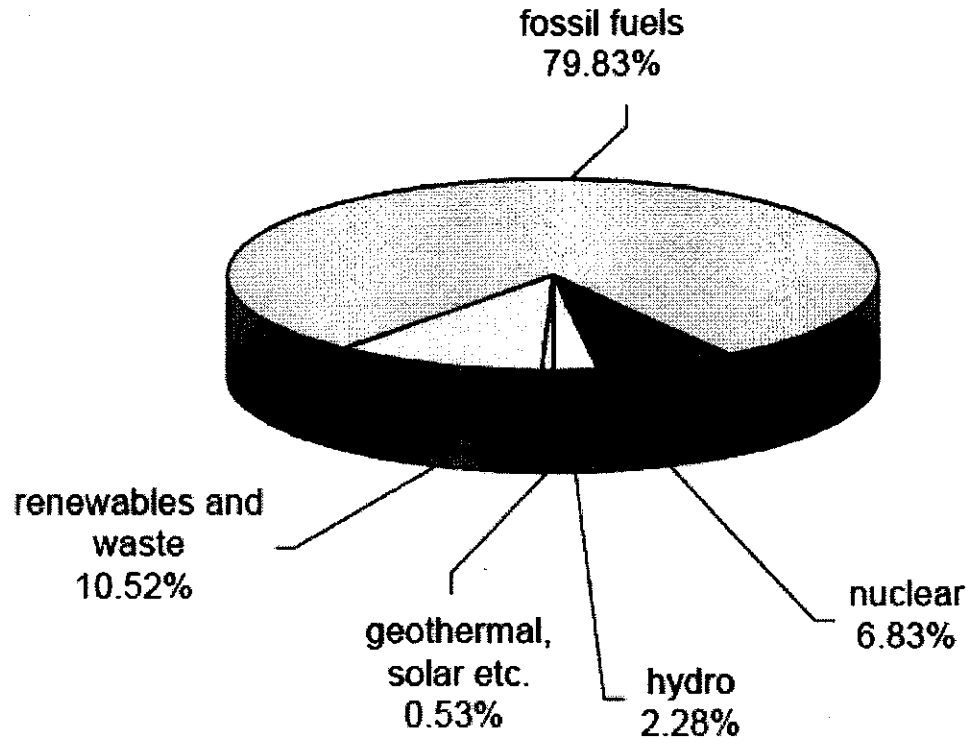

Fig. 1.1 World share of primary energy supply in 2000.

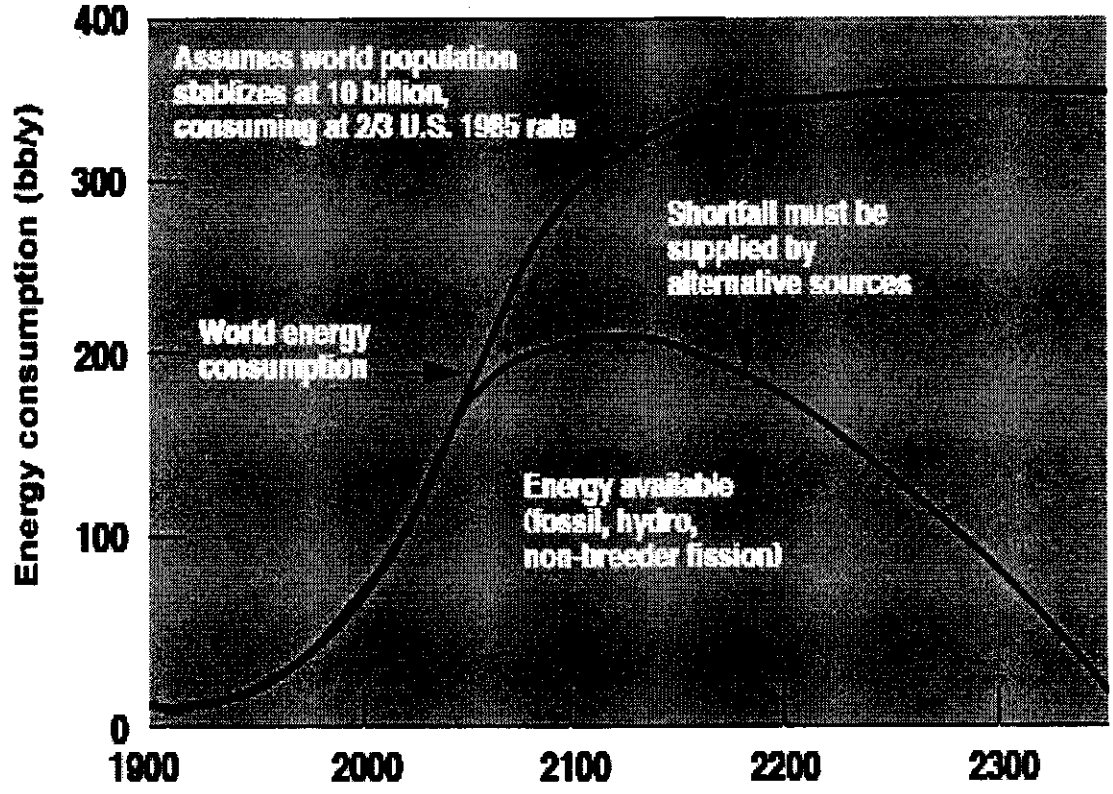

Fig. 1.2 The word energy consumption demand and the energy available

1.1.2 Fusion energy

In a fusion reaction, two light atomic nuclei combine to form heavier nuclei with the simultaneous release of energy. The release of fusion energy is in accordance with the Einsten's mass-energy relation:

$$E = mc^2$$

Where E is energy, M is mass and c is the velocity of light. The mass loss in fusion process is converted into energy.

The fusion energy is the source of the sun and the stars. The fusion reaction in the sun and the stars is confined by the gravitation force. On

earth the confinement of fusion reaction by the gravitation force cannot be realized because the gravitation force is too low [13]. Hence, two alternative ways, namely Magnetic Confinement Fusion (MCF) and Inertial Confinement Fusion (ICF) have been investigated to achieve the controlled fusion reactions on earth. However, there is a major technical difficulty. All nuclei are charged and initial amount of kinetic energy is needed to increase their probability of penetrating the Coulomb barrier, which, normally, keeps them apart and prevents the fusion reaction from taking place. When fusion is driven by heat energy, the process is called thermonuclear fusion [14].The atoms of fuel for the thermonuclear fusion reaction must be heated to very high temperatures (100 million degrees) so that they should be ionized (forming a plasma) and have sufficient energy to overcome the Coulomb resistance.

MCF uses strong magnetic fields to confine the nuclei which are heated by neutral beam injection heating, ohmic heating, microwaves heating, etc. ICF uses powerful energy beams, such as lasers, to compress and heat the fuel to fusion temperatures. The inertia of the fuel itself is used to confine it long enough for the necessary fusion reaction to occur.

1.2 Fusion reactor and blanket

The most commonly considered fuel cycles for fusion reactor are D-T, D-D, and D-^{3}He. The primary reactions in the three fuel cycles are:

$$D + T \rightarrow {}^4He\ (3.5\ MeV) + n\ (14.1\ MeV)$$

$$D + D \rightarrow {}^3He\ (0.8\ MeV) + n\ (2.6\ MeV)$$

$$D + D \rightarrow T\ (1.0\ MeV) + p\ (3.0\ MeV)$$

$$D + {}^3He \rightarrow {}^4He\ (3.7\ MeV) + p\ (14.7\ MeV).$$

Figure 1.3 shows the cross sections of these reactions as the function of energy [15]. It can be seen that the D-T reaction has the largest cross section. So the fusion with D-T fuel cycle is the easiest way to be realized.

Here most of the present study on fusion reactor designs focuses on the D-T reaction system.

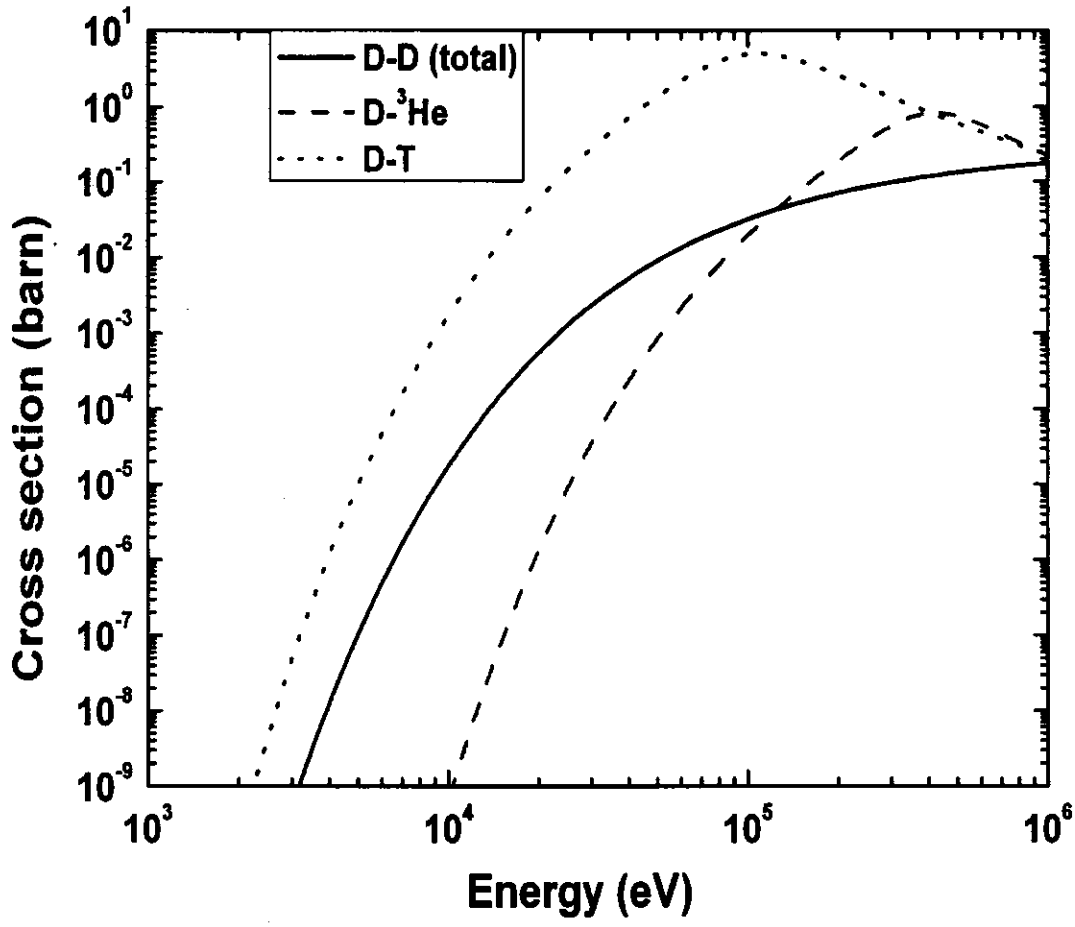

Fig. 1.3 Cross section vs. energy

Figure 1.4 shows a schematic view of the concept of MCF fusion reactor. Plasma is confined in a designed region by a strong magnetic field. In the D-T reaction, the output reaction energy of 17.6 MeV appears as a 14.1 MeV neutron and a 3.5 MeV α particle. The energy of 3.5 MeV α -particle is used to heat the core plasma for sustaining self-ignition. Hence 80% of the reaction energy in D-T fuel cycle is carried by the 14.1 MeV neutrons. Since the neutrons carry the main source of recoverable energy, they must be absorbed in a region surrounding the plasma, referred to as the blanket, as

shown in Fig 1.4. Converting the kinetic energy of 14.1 MeV neutrons into heat through the neutron interaction with materials and transferring the heat to the external thermal cycle is one of the major functions of the blanket.

In addition, tritium with a half life of 12.3 years does not exist naturally. So it must be bred through the neutron reactions with lithium in the blanket. The reactions are:

$$n + {}^{6}Li \rightarrow T + {}^{4}He + 4.79\ MeV$$

$$n + {}^{7}Li \rightarrow T + {}^{4}He + n - 2.47\ MeV.$$

The permanent components need an efficient shield from the neutron and photon radiation to achieve high economy of fusion reactor. A shielding region, surrounding the breeding region, is required to provide the necessary protection for the vacuum vessel and external components. The primary function of the shielding region is for the magnet, which should be superconducting magnets for steady-state operation at high magnetic fields. The life of superconducting magnets are limited by total fluences for radiation damages with neutrons and γ-rays.

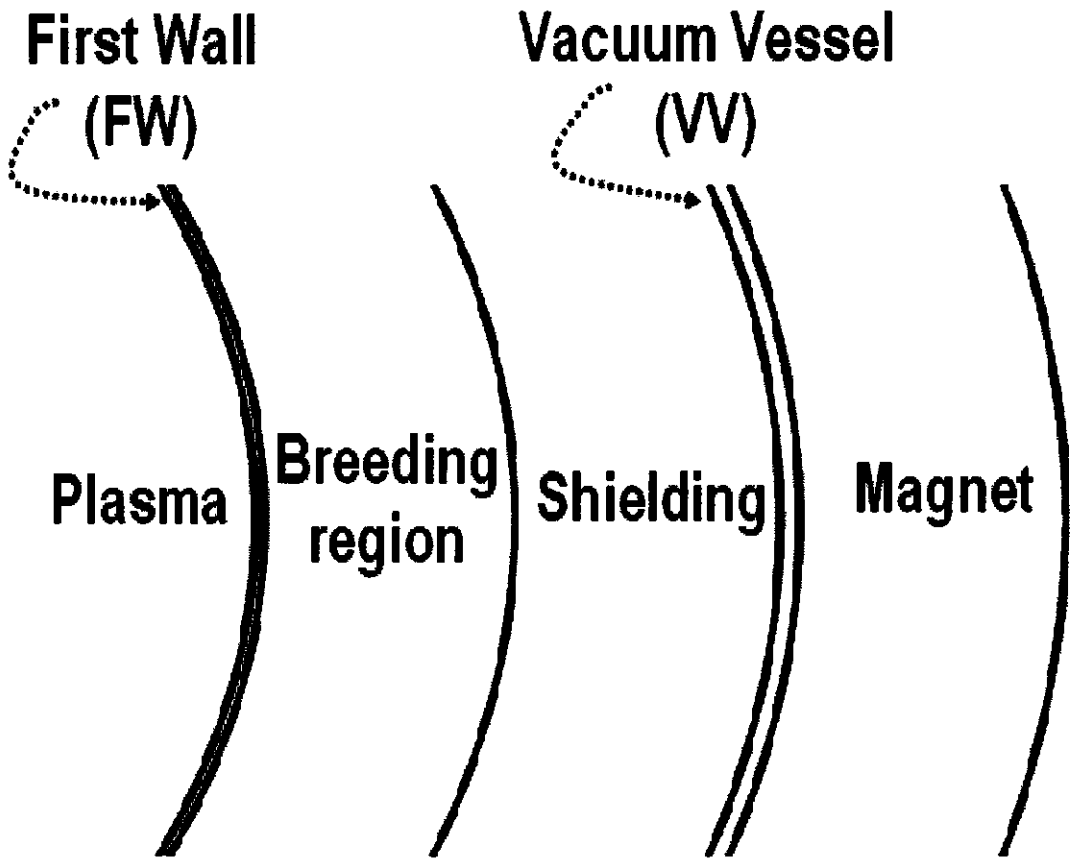

Fig. 1.4 Schematic view of blanket

The main functions of the blanket of D-T fusion reactor can be summarized as follow:

1. Converting the kinetic energy of D-T neutrons into heat and removing the heat,
2. Breeding tritium,
3. Shielding.

Now a tokomak type International Thermonuclear Experimental

Reactor (ITER) is under design. ITER is the first experimental fusion reactor and is expected to have its first plasma at 2016 [16-25]. The cutaway and the major plasma parameters and dimension of ITER were shown in Fig. 1.5 and Table1.1 [20], respectively.

The objective of ITER is to demonstrate the scientific and technological feasibility of fusion energy for commercial energy production and to test the technologies for a demonstration fusion power plant [20, 21, 25]. ITER will accomplish this by demonstrating controlled ignition and extended burn of deuterium-tritium plasma in a tokamak confinement; with steady state as an ultimate goal, by demonstrating technologies essential to reactor in an integrated system, and by performing integrated testing of the high-heat-flux and nuclear components required to utilize fusion energy for practical purposes [18,20].

The ITER basic device has shielding blankets only. ITER expects to use tritium supplied from external sources instead of breeding tritium itself. However the next-generation reactors (DEMO) and commercial reactors will require tritium breeding self-sufficiency. ITER has the mission to test design concepts of tritium breeding blankets relevant to DEMO. Breeding blankets concepts will be tested in ITER by inserting Test Blanket Modules (TBM) in specially designed ports [26]. Three of the equatorial ports are dedicated for blanket test modules.

Objectives for TBM testing in ITER are [26-31]:

- Validate of structural integrity and theoretical predictions under combined and relevant thermal mechanical and

electromagnetic loads

- Demonstrate tritium breeding performance and on-line tritium recovery
- Demonstrate high-grade heat extraction
- Demonstrate integral performance of blanket system
- Validate computational tools and data used in neutronics blanket design.

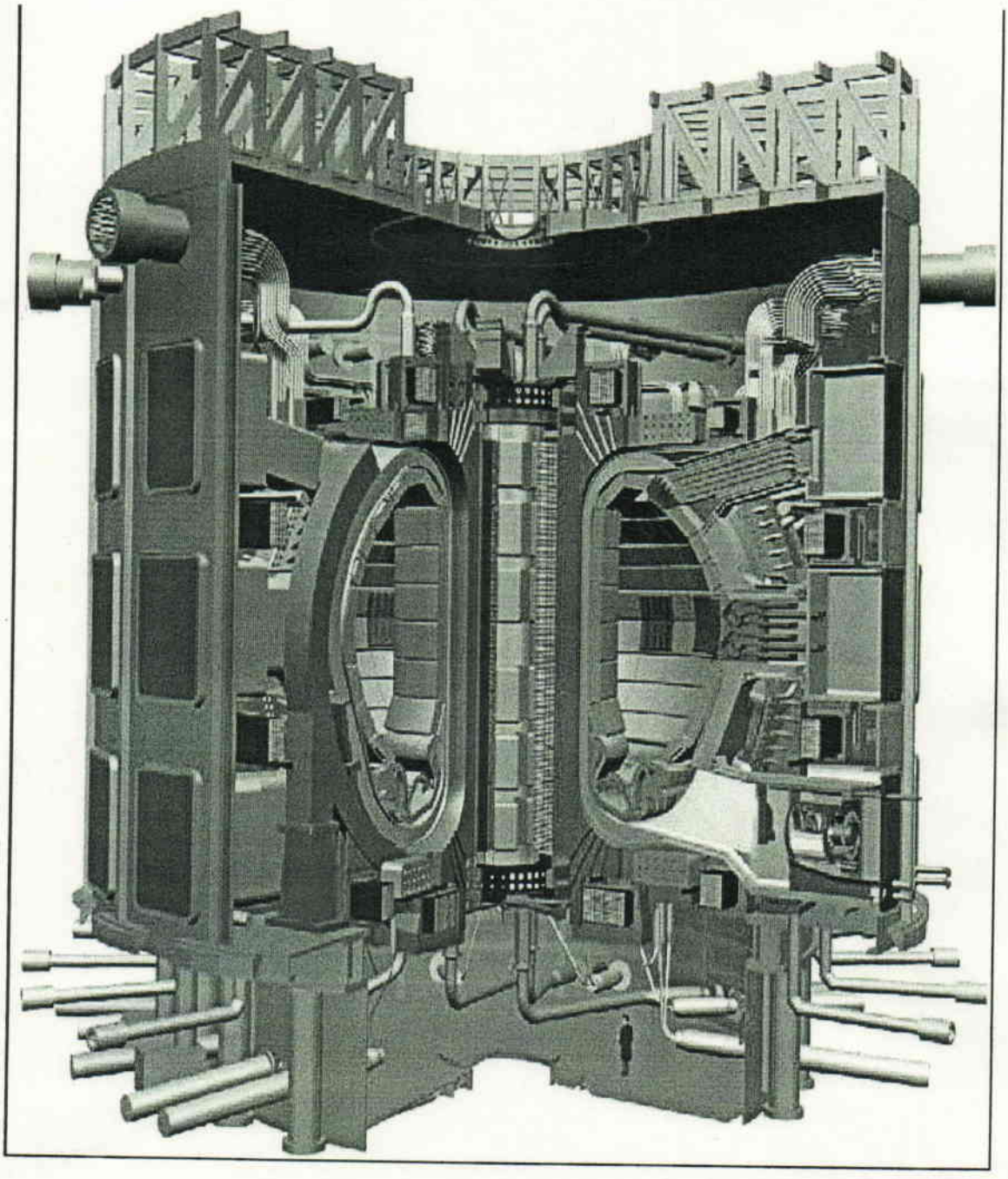

Fig. 1.5 A cutaway of ITER

Table 1.1 Main Plasma Parameters and Dimensions

Total Fusion Power	500 MW *(700 MW)*
Q – fusion power/additional heating power	≥10
Average 14MeV neutron wall loading	0.57 MW/m^2 *(0.8 MW/m^2)*
Plasma inductive burn time	≥400 s
Plasma major radius (R)	6.2 m
Plasma minor radius (a)	2.0 m
Plasma current (I_p)	15 MA *(17 MA*)*
Vertical elongation @95% flux surface/separatrix (κ_{95})	1.70/1.85
Triangularity @95% flux surface/separatrix (δ_{95})	0.33/0.49
Safety factor @95% flux surface (q_{95})	3.0
Toroidal field @6.2 m radius (B_T)	5.3 T
Plasma volume	837 m^3
Plasma surface	678 m^2
Installed auxiliary heating/current drive power	73 MW**

* The machine is capable of a plasma current up to 17MA, with the parameters shown in parentheses) within some limitations over some other parameters (e.g., pulse length).

**A total plasma heating power up to 110MW may be installed in subsequent operation phases.

1.3 Candidate blanket materials and blanket concepts

The fusion blanket is composed of:

- Tritium breeder (solid or liquid)
- Structural materials
- Neutron multiplier (optional)
- Coolant (helium, water, liquid metal, molten salts).
- Shielding

The materials proposed by blanket designers are briefly presented here.

1.3.1 Structural materials

The structural materials for fusion device need to have very good radiation resistance as well as low activation properties. Present three leading candidates for first wall and blanket are reduced activation ferritic martensitic (RAFM) steels, vanadium alloys and SiC/SiC composites. RAFM steels, which mainly consist of Fe, Cr, W, Mn, V instead of Mo, Ni and Nb, have the most advanced technological base of the three candidate materials. However the operating temperature is limited to 550 °C mainly due to the strong reduction in mechanical strength. The possible improvement with oxide dispersion (ODS) has been investigated [32]. Vanadium alloys exhibit high operating temperature (700 °C), better corrosion resistance in lithium, and good radiation damage resistance [33,34]. In addition, the vanadium alloy is inherently low activation. Recent efforts on vanadium alloy

development have been focused on characterizing V-4Cr-4Ti [35-37]. Main issues on V-alloy are irradiation effects, influence of environmental impurities, etc. [33]. SiC/SiC composites could allow very high operating temperature to ~1000 °C. Additional attractive feature is the low afterheat with irradiation. On the other hand, SiC/SiC composites are still the least-developed of the three candidate materials and several issues are remaining, such as fabrication of massive component, hermetic joining, radiation induced swelling and creep, and radiation induced degradation of thermal conductivity [32-33, 38-40].

1.3.2 Breeder materials

The most efficient reactions for breeding tritium are the neutrons with ^{6}Li and ^{7}Li. The natural abundance (atom %) of ^{6}Li and ^{7}Li is 7.59% and 92.41%, respectively. Figure 1.6 shows the possible tritium breeding reaction with lithium isotopes. The most favorable breeding reaction is $^{6}Li(n, t)$, which has high cross section with thermal neutrons. Another reaction is $^{7}Li(n, nt)$ with about 2.5 MeV threshold energy. It is worth noticing that the $^{7}Li(n, nt)$ is quite important as the "neutron multiplication reaction" from viewpoint of tritium breeding since the product neutron can potentially result in another tritium.

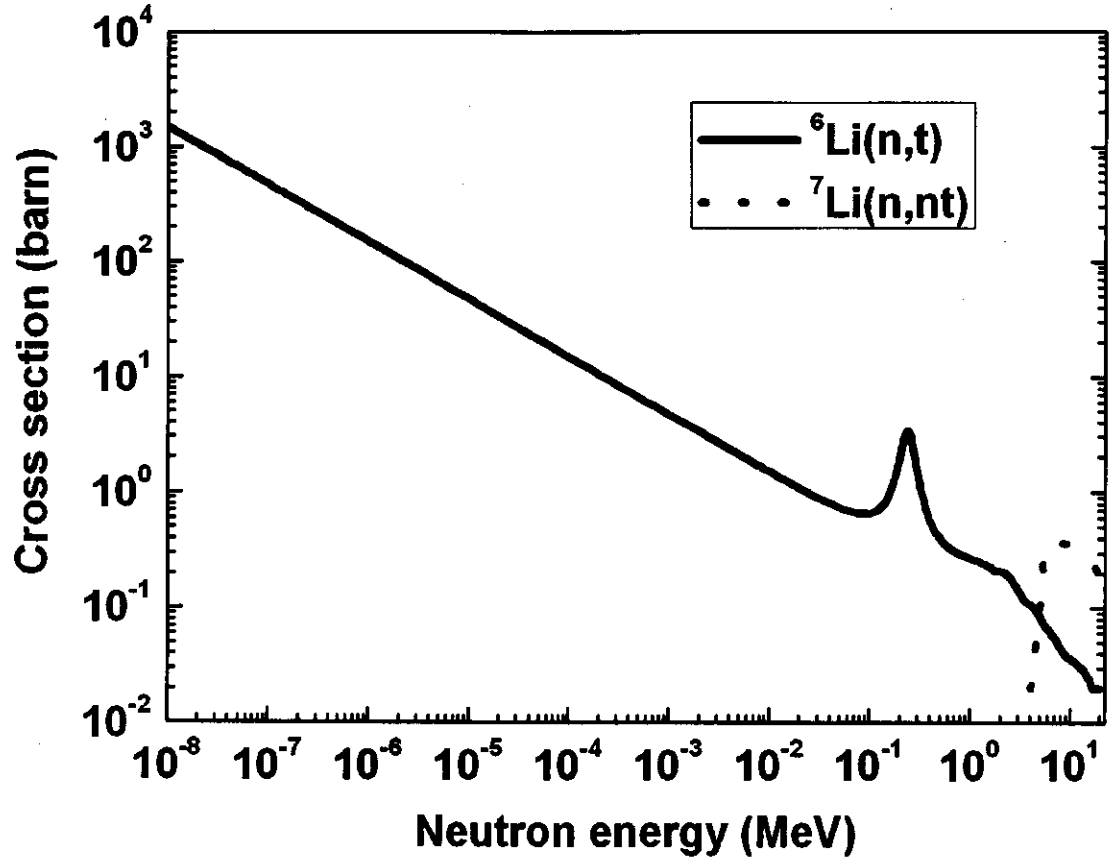

Fig. 1.6 ^{6}Li(n, t) and ^{7}Li(n, nt) cross sections.

Table 1.2 presents the typical properties of the selected candidate ceramic breeding material [41]. The Li-based ceramic breeders have high thermal stability and chemical inertness. However, they have poor mechanical strength and thermal properties. It is difficult to precisely control the temperature of the breeders due to their low thermal conductivity. Recently Li_2ZrO_3 and Li_2TiO_3 were selected as the breeder materials for the TBM of ITER project due to their excellent tritium release behavior at low temperature [42,43].Thermal conductivity values for Li_2TiO_3 are

intermediate between those for $LiAlO_2$ and Li_2ZrO_3 [44]. The critical design issue for solid breeders is the changes of mechanical properties with long-term irradiation at high temperature and under large temperature gradients.

Liquid breeders are immune to radiation damage. The liquid breeder can be circulated inside and outside the blanket, so continuous tritium extraction can be performed outside the blanket. Maintenance of the liquid breeder is easier compared to the solid breeder. Critical issues associated with liquid breeders are the compatibility with structural materials and serious MHD pressure drops when metallic breeders, e.g. Li and LiPb flow in high magnetic field [45-48]. The comparison of the properties of selected candidate liquid breeder is shown in Table 1.3 [49]. The attractive advantages of lithium include: low activation, high tritium breeding property, high thermal conductivity, low melting point and good tritium solubility. Contrary to Flibe and LiPb, the high tritium solubility of lithium results in good tritium containment and small permeation losses through structural materials. However, R&D on tritium recovery is one of issues. The issue related to safety for lithium is the chemical reactivity with water and air. Key features of LiPb include: high density, reduced reactivity with air and water compared to lithium, and low tritium solubility resulting in low tritium inventories and relatively high pressure. For Flibe the MHD pressure drop issue is not serious due to the low electrical conductivity. Also Flibe has the attractive features of low chemical reactivity with water and air, small density change on melting, low activation and good neutron

attenuation property. However Flibe has the low thermal conductivity and relatively high viscosity that lead to lower heat transfer capability. In addition, the tritium permeation is a serious issue because of the low tritium solubility in Flibe.

Table 1.2 Typical properties of candidate ceramic breeding material (at 500 °C)

	Li_2O[$]	$LiAlO_2$[$]	Li_2ZrO_3[$]	Li_4SiO_4[**]
Li density (g cm^{-3})	0.75	0.22	0.30	0.53
Melting point (°C)	1430	1750	1615	1255
Saturation temperature (°C) at				
10^{-2} Pa total partial pressure	1020	1270	>1350	<1120
Thermal conductivity (W/mK)	4	2.8	1.4	1.4
Lin. Thermal expansion				
Coef. (10^{-6}/°C)	29	12	11	30
Young modulus (GPa)	60	75	90	85
Ultim. Bending strength (MPa)	80	60	60	50
Temperature (°C) corresponding to				
a tritium residence time of 1 day	325[*]	430	310	380

[$] 1 μm grain diameter, 20% porosity.

[*] 10 μm grain diameter.

[**] 25 μm grain diameter, 3% porosity.

Table 1.3 Comparison of liquid breeders

	Li	Pb-17Li	Li_2BeF_4
Melting point (°C)	180	235	459
Density (g cm^{-3})	0.48	8.89	2.0
Li density (g cm^{-3})	0.48	0.062	0.28
Breeding property	Good	Fairly good	Neutron multiplier required
Chemical reactivity	Active	Middle	Almost stable
Tritium solubility	High	Very low	Very low

1.3.3 Coolant materials

Various coolants have been proposed for fusion blanket such as: helium, water, liquid metal, and molten salt (Flibe).

The main advantages of helium as blanket coolant are total transparency to neutrons and chemical inertness. There is also no MHD consideration for helium because of its nonconductive properties [41,50]. The principal disadvantage is its low volumetric heat capacity, which leads to the need to operate the helium pressure in the range of 4-8 MPa [34,41] and a high flow rate. Thus, higher pumping power is required compared to water.

Water systems have been used extensively in fission nuclear powers, e.g., pressurized water in PWRs. Water has a good materials compatibility data base and excellent heat transfer characteristics and is very low in price [34]. However, high pressure is required for high temperature operation to achieve high thermal energy conversion efficiency. There is safety concern of

water in some designs with Be as neutron multiplier because of the production of H through the reaction of Be with water at above 600 ℃.

The liquid Li, LiPb, or Flibe also can serve as coolant and tritium breeder in blanket design. In these cases, the heat transfer process would be simple because the most heats are produced in coolant. The crucial issue of MHD for Li or LiPb can be remarkably alleviated by the use of electrical insulator coating between Li or LiPb and flowing channels [45-47].

1.3.4 Neutron multiplier materials

Beryllium and lead are the proposed neutron multiplier materials for fusion blankets. Figure 1.7 shows the neutron multiplying cross section of ^{9}Be and ^{208}Pb. ^{208}Pb has high cross section at 14 MeV, 2.15 barn. Since its reaction threshold is about 7.41 MeV and Q = -7.37 MeV, the energy of the secondary neutrons emitted in a (n, 2n) reaction are below threshold and is not enough to induce a further (n, 2n) reaction. Although ^{9}Be has lower cross section than ^{208}Pb, beryllium is better multiplier because of its lower threshold, about 1.75 MeV and Q = -1.57 MeV. The energy of the secondary neutrons emitted from ^{9}Be(n, 2n) reaction exceed the threshold and can induce a further (n, 2n) reaction. Beryllium is also a good neutron moderator with very low absorption of thermal neutrons. Beryllium can be both as neutron multiplier and moderator in a fusion blanket.

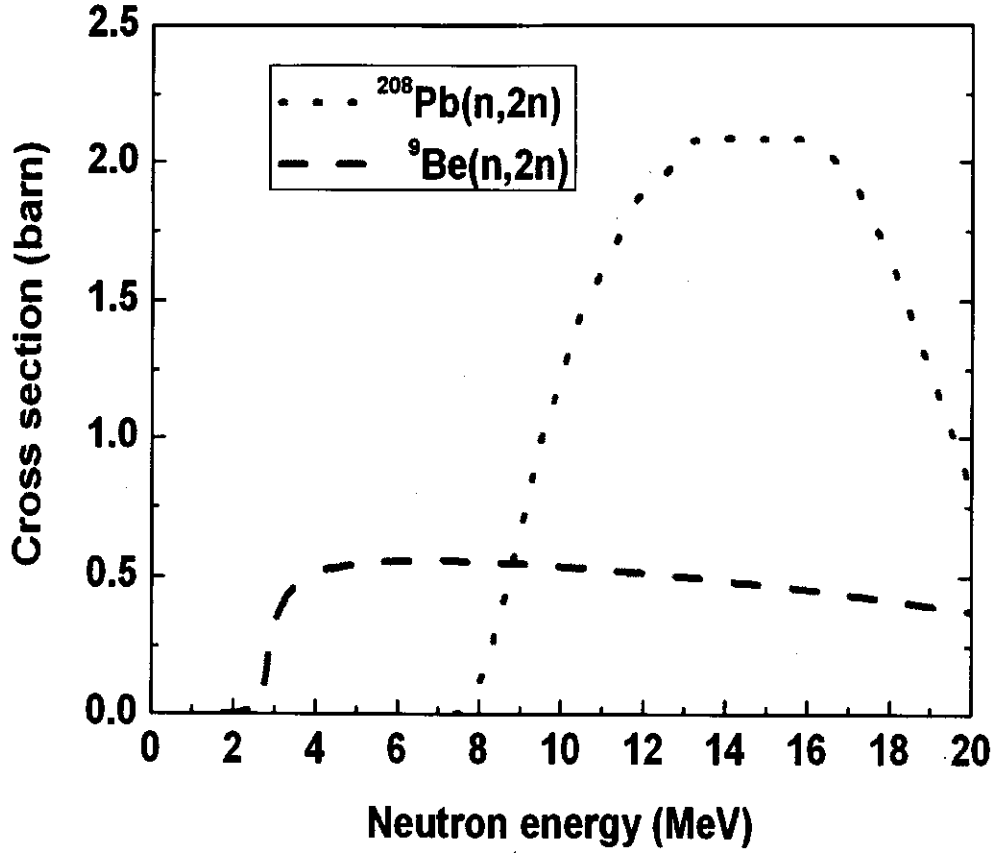

Fig. 1.7 ^{208}Pb(n, 2n) and ^{9}Be(n, 2n) cross sections.

Both beryllium and lead can meet the neutron multiplication requirement of fusion blankets. The main concerns for beryllium are the resource limitation and irradiation swelling [34]. Low melting point (325 °C) and its volumetric expansion are the main design issue for the use of lead in fusion blankets [41].

It should be noted here that lithium can potentially achieve tritium self-sufficiency by the reaction:

$$n + {}^{7}Li \rightarrow T + {}^{4}He + n' \quad - 2.47\ MeV$$

In this reaction, tritium is generated without consuming neutron. The contribution to tritium production with this reaction largely depends on the ^{7}Li density in lithium because of the low cross section and the high energy threshold (2.5 MeV) as shown in Fig. 1.6.

1.3.5 Shielding materials

Heavy materials with a relatively large inelastic cross section e.g., steel, should be used in shielding region to reduce energy of the high energy neutrons. However the heavy materials are inefficient shielding materials below the inelastic threshold. A good material for neutron capture in this energy region is B_4C. ^{10}B has a large (n, α) reaction for low energy neutrons only releasing soft gamma (0.5 MeV) compared to the hard gamma emission with (n, γ) capture in other materials. The B_4C can efficiently moderate and absorb neutrons at low energy. Since the high cost of B_4C limits their use in large quantities, the optimization of the mixture of B_4C and heavy materials is necessary from the viewpoint of economy.

1.3.6 Proposed blanket concepts

The proposed candidates of the blanket components (coolant, tritium breeder, shielding materials, and structure materials) are listed in Table 1. 4. The selections of components for blanket design need consideration of the compatibility of different components from chemical, thermal and safety standpoints.

The blanket concepts can be categorized into liquid blanket and solid

blanket according to the tritium breeder. Various blanket concepts have been proposed. However, each blanket concept has its advantages and drawback. Several blanket design options being proposed are listed below [30, 51-56]:

- ✧ Helium-cooled Ceramic/Be
- ✧ Water-cooled Ceramic/Be.
- ✧ Self-cooled liquid Li with V-alloy.
- ✧ Helium-cooled or dual coolant LiPb.
- ✧ Self-cooled or dual coolant Molten Salt

Table 1.4 Candidate components of blanket.

Breeder	solid	Li_4SiO_4, Li_2TiO_3, Li_2ZrO_3, LiO_2, $LiAlO_2$
	liquild	Li, Li Pb, Flibe, Flinabe
Neutron multiplier		Be, Pb
Structural materials		SS-316, RAFM (F82H, JLF1, EUROFER, CLAM), SiC, V- alloy
Coolant		He, H_2O, Pb-Li, Flibe, Li
Shielding materials		B_4C, WC

1.4 FFHR design

Helical magnetic configuration is an advanced magnetic confinement system with current-less and natural divertor and can simplify structure with potential of force-free reactors [57]. Relative to tokomak devices, helical devices exhibit advantages [58,59]:

- Steady state operation with a small fraction of recirculating power,
- Plasma operation with no dangerous current disruptions.

The large helical device (LHD) was constructed in the National Institute for Fusion Science (NIFS) in 1998. Force-free helical reactor (FFHR) is D-T DEMO-reactor design based on LHD. The force-free configuration would allow to simplify the coil supporting structure or to use high magnetic field instead of high plasma β [58]. There are a series of FFHR designs, namely FFHR-1, FFHR2, FFHR2m1, and FFHR2m2. The schematic view of FFHR2m1 is shown in Fig. 1.8 [60]. The main design parameters of FFHR designs were summarized in Table 1.5 [61-62].

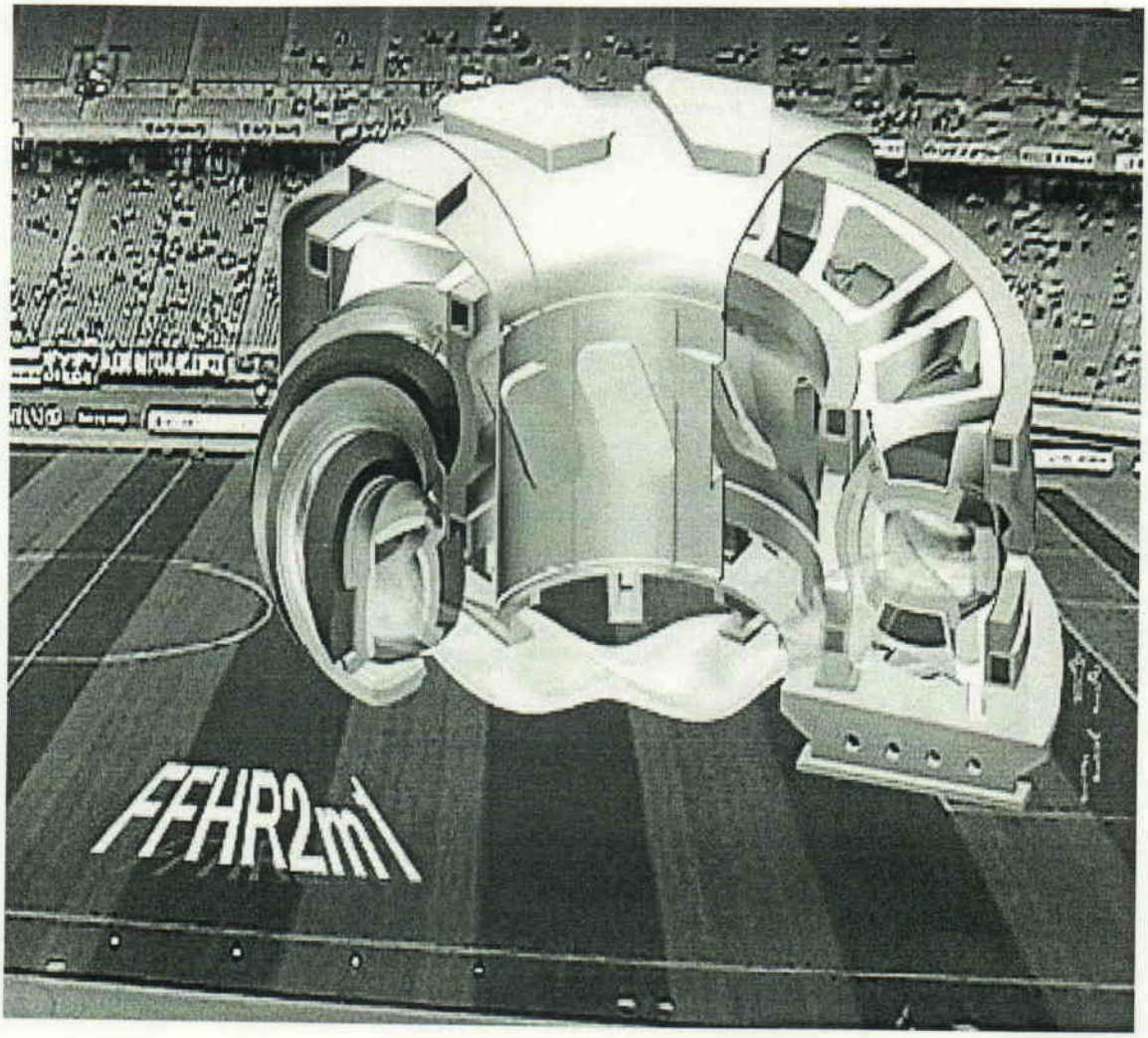

Fig. 1.8 Schematic view of FFHR2m1

Table 1.5 Design parameters of LHD and series of FFHR designs

Design Parameters	LHD	FFHR-1	FFHR2	FFHR2m1	FFHR2m2
Polarity, l	2	3	2	2	2
Field periods, m	10	18	10	10	10
Coil pitch parameter, γ	1.25	1	1.15	1.15	1.25
Coil major radius, Rc (m)	3.9	20	10	14.0	17.3
Coil minor radius, a_c (m)	0.98	3.33	2.3	3.22	4.33
Plasma radius, a_p (m)	0.61	2	1.2	1.73	2.80
Blanket space, ∇(m)	0.12	1.1	0.7	1.2	1.1
Magnetic field, B_0 (T)	4	12	10	6.18	4.43
Maximum field on coils, B_{max} (T)	9.2	16	15	13.3	13.0
Coil current density, j (MAm^{-2})	53	27	25	226.6	32.8
Magnetic energy (GJ)	1.64	1290	147	120	142
Fusion power (GW)		3	1	1.9	3
Neutron wall load (MWm^{-2})		1.5	1.5	1.5	1.3
External heating power, P_{ext} (MW)		100	70	80	100
α heating efficiency, $\eta\alpha$		0.7	0.7	0.9	0.9
Effective ion charge, Zeff		1.5	1.40	1.34	1.35
Electron density, $n_e(0)$ (10^{19} m^{-3})		20.0	27.4	26.7	19.0
Plasma beta, $<\beta>$ (%)		0.7	1.6	3.0	4.1

Self-cooled Flibe blanket with Be as neutron multiplier and JLF1 as the structure materials has been proposed for FFHR2 design [61].The new design of FFHR2, FFHR2m1 and FFHR2m2, are proposed to solve the key engineering issues of blanket space limitation and replacement difficulty [62]. The available space for blanket in FFHR2m1 has been extended to 1.2 m. Therefore it is possible to explore other blanket design options for FFHR2m1 than Flibe/Be/JFL1. The thermal efficiency of the plant is relatively low due to high melting point of Flibe (~430 °C) and the limit of maximum operation temperature of JLF1(~550 °C). On the other hand, vanadium alloy (V-alloy) has superior thermal-mechanical properties and can be operated up to ~700 °C [33]. So the blanket with the structure materials of V-alloy has potentiality for higher thermal efficiency.

For blankets using V-alloy, liquid Li and Flibe were proposed as candidate liquid tritium breeders [63,64]. Liquid Li is an attractive breeding material due to high Li content, high thermal conductivity and good compatibility with V-alloy to high temperature. However the flow of Li in magnetic field would cause an issue of MHD pressure drops [63]. The application of MHD insulator coating, e.g. Er_2O_3 [65-66], is necessary for Li blanket.

Flibe posses several attractive features such as low electric conductivity and low reactivity with water and air. The deposition of WF_6 or MoF_6 into Flibe was proposed for Flibe/V-alloy option to reduce tritium inventory in structure components and to plate the wall with anticorrosive W or Mo [64,67]. Two self-cooled blanket concepts of Li/V-alloy (Li/V) and

Flibe/V-alloy (Flibe/V) blankets without external neutron multiplier Be were investigated for FFHR2m1 such as assessment of Tritium Breeding Ratio (TBR) and shielding of Li/V and Flibe/V blankets [67,68]. Russia is proposing Li/V blanket with Be (Li/Be/V) concept for enhancing TBR [54]. The original FFHR2m1 design also proposed Flibe with external Be. Thus Flibe/V blanket with external Be (Flibe/Be/V) can also be a candidate. Because of the neutron spectral difference, the neutronics issues may be different for the Li/Be/V and Li/V and for the Flibe/V and Flibe/Be/V blankets.

1.5 Neutronics design issues and the objectives of the present study

In a D-T fueled fusion reactor, intensive D-T neutrons give rise to a variety nuclear effects which strongly affect the blanket design. Blanket design issues associated with D-T neutrons are: irradiation damage, tritium breeding, activation, energy production, shielding, safety & environment, etc.

The general neutronics design requirements of blanket including shielding are listed as follow:

- Blanket, especially first wall (FW), should be resistant to radiation damage
- The tritium breeding ratio (TBR) needs to be exceed unity
- The blanket should efficiently convert the kinetic energy of neutrons into heat
- The blanket including shielding must attenuate neutron flux and γ -ray to accept level for vacuum vessel (VV) and magnet
- The materials utilized in blanket should have low activation properties.

The neutronics issues need to be assessed for blanket including shielding with respect to TBR, nuclear heating, fast neutron and γ -ray flux in magnet, and radioactivity etc. Neutronics analysis is a fundamental prerequisite for the nuclear design of fusion reactor systems. The codes and nuclear data used in neutronics analysis play an important role in characterizing the economy and safety of blanket system.

The present modified FFHR2 design, FFHR2m1, has been designed with the lifetime of 30 years and the fusion output power of 1.9 GW. The plasma major and minor radius of FFHR2m1 is 14 and 1.73 m, respectively. The average neutron wall loading is 1.5 MW/m^2. The space for blanket is limited in FFHR2m1. Maximum thickness for blanket including shielding is 1.2 m. The design requires detailed neutronics examinations. Key design goals for FFHR2m are: an overall tritium breeding ratio (TBR) of ~1.1 (local ~ 1.3) and fast neutron fluence (>0.1 MeV) at superconducting magnet with 30 years operation is less than 10^{19} n/cm^2.

Li or Flibe blanket is the candidate breeding and coolant materials for FFHR2m design. Be is a potentially necessary neutron multiplier. Be is also an excellent neutron moderator with low absorption cross section for thermal neutrons. Use of Be is an option for both Li and Flibe blankets for FFHR2m although there are some issues specific to Be such as resource limitation and irradiation effect (swelling). It is necessary to apply an electrical insulating coating e.g. Er_2O_3, for Li blanket to solve the Magneto-Hydro Dynamic (MHD) pressure drops when Li flows in strong magnetic field. The effect of Be and MHD coating (Er_2O_3) need to be examine with respect to TBR, shielding and activation in FFHR2m condition. The activation issues of Flibe in FFHR2m condition are also needed to be investigated.

However the nuclear data bases of Flibe and Er in fusion environment are limited. To provide viable design, the neutronics analysis procedure including transport and activation codes and libraries applied to liquid blanket need to be verified or improved. For this purpose, systematic

comparison of calculation and experiment is necessary.

The objectives of the present study are:

A) To investigate Li and Flibe blankets for FFHR2m by neutronics analysis with respect of TBR, shielding and activation.

B) To examine or improve the neutronics calculation procedure for application to liquid blankets by comparison with activation experiment with D-T neutrons.

CHAPTER 2

Neutronics and activation codes

The most important characteristic of any fusion blanket and shield design is its response to irradiation by the 14 MeV fusion neutrons. In order to calculate this response, the codes simulating transport of neutrons and photons must be utilized. The codes will provide such information as the neutron flux and spectrum as a function of position within the blanket, the volumetric heating of different blanket regions, and the local and overall tritium breeding ratio of the blanket. The methods available to simulate the transport of neutron of gamma can be classified into two broad groups: deterministic method and statistical based method. The comparison of two methods is shown in Table 2.1. The code based on Monte Carlo method, MCNP-4C was chosen for the present analysis due to the complex geometry of FFHR based on helical configuration. A brief description of MCNP-4C codes was provided in Section 2.1.

Activation of the components will occur in D-T fueled fusion power plants due to the interaction of the neutrons with the materials constituting the devices. Several parameters have been used to assess the relevance of the activation to safety and waste disposal issues, activity, contact γ-dose rate, decay power and potential biological hazard. In this study, the activation analysis was performed using an inventory code of FISPACT-2001. It is a well verified and validated code [69]. A brief description of FISPACT-2001 code was presented in Section 2.2.

Table 2.1 Comparison of deterministic and statistical Monte Carlo approach

Deterministic approach	Statistical Monte Carlo approach
Advantage - Spatial resolution - Full map of all mesh points	Advantage - Exact geometry representation - Continuous energy treatment of cross section
Disadvantage - Group treatment of energy variation - Limited to simple calculation model	Disadvantage - Results with statistical error - Consuming CPU time

2.1 MCNP and the Monte Carlo method [70]

Monte Carlo can be used to duplicate theoretically a statistical process (such as the interaction of nuclear particles with materials) and is particularly useful for complex problems that cannot be modeled by computer codes that use deterministic methods. The individual probabilistic events that comprise a process are simulated sequentially. The probability distributions governing these events are statistically sampled to describe the total phenomenon. In general, the simulation is performed on a digital computer because the number of trials necessary to adequately describe the phenomenon is usually quite large. The statistical sampling process is based on the selection of random numbers—analogous to throwing dice in a

gambling casino—hence the name "Monte Carlo." In particle transport, the Monte Carlo technique is pre-eminently realistic (a numerical experiment). It consists of actually following each of many particles from a source throughout its life to its death in some terminal category (absorption, escape, etc.). Probability distributions are randomly sampled using transport data to determine the outcome at each step of its life.

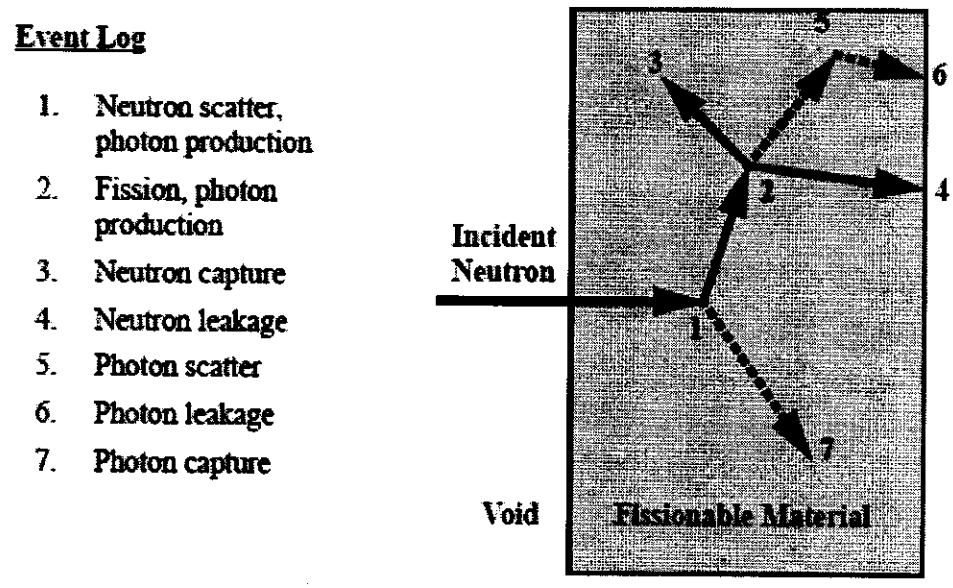

Fig. 2.1 Representation of the random history of an incident neutron in a slab of material that can undergo fission

Figure 2.1 represents the random history of a neutron incident on a slab of material that can undergo fission. Numbers between 0 and 1 are selected randomly to determine what (if any) and where interaction takes place, based on the rules (physics) and probabilities (transport data) governing the processes and materials involved. In this particular example, a neutron collision occurs at event 1. The neutron is scattered in the direction shown, which is selected randomly from the physical scattering distribution.

A photon is also produced and is temporarily stored, or banked, for later analysis. At event 2, fission occurs, resulting in the termination of the incoming neutron and the birth of two outgoing neutrons and one photon. One neutron and the photon are banked for later analysis. The first fission neutron is captured at event 3 and terminated. The banked neutron is now retrieved and, by random sampling, leaks out of the slab at event 4. The fission-produced photon has a collision at event 5 and leaks out at event 6. The remaining photon generated at event 1 is now followed with a capture at event 7. Note that MCNP retrieves banked particles such that the last particle stored in the bank is the first particle taken out.

This neutron history is now complete. As more and more such histories are followed, the neutron and photon distributions become better known. The quantities of interest (whatever the user requests) are tallied, along with estimates of the statistical precision (uncertainty) of the results.

MCNP-4C is a general-purpose Monte Carlo N-Particle code that can be used for neutron, photon, electron, or coupled neutron/photon/electron transport, including the capability to calculate eigenvalues for critical systems. Pointwise cross-section data are used. For neutrons, all reactions given in a particular cross-section evaluation (such as ENDF/B-VI) are accounted for. Thermal neutrons are described by both the free gas and S(α, β) models. For photons, the code takes account of incoherent and coherent scattering, the possibility of fluorescent emission after photoelectric absorption, absorption in pair production with local emission of annihilation radiation, and bremsstrahlung.

Important standard features that make MCNP-4C very versatile and easy to use include a powerful general source, criticality source, and surface source; both geometry and output tally plotter; a rich collection of variance reduction techniques; a flexible tally structure; and extensive collections of cross-section data.

2.2 FISPACT-2001 [71-74]

FISPACT is an inventory code that has been developed for neutron induced activation calculations for materials in fusion devices. It is a powerful code that can answer the basic questions about the numbers of atoms and the activity in a material following neutron irradiation, and also give details of the pathways by which these nuclides are formed. It can treat trace amounts of actinides that are able to fission, and includes the effects of sequential charged particle reactions.

The core task of FISPACT is the solution of a set of differential equations that describe the amounts of atoms of various nuclides present following the irradiation of a given material in a neutron field. The set of differential equations is given in equation 2.1. .

$$\frac{dN_i}{dt} = -N_i(\lambda_i + \sigma_i\Phi) + \sum_{j \neq i} N_j(\lambda_{ij} + \sigma_{ij}\Phi) + S_i$$

$$S_i = \sum_k N_k \sigma_k^f \Phi Y_{ik} \qquad (2.1)$$

Where

N_i is the amount of nuclide i at time t

λ_i is the decay constant of nuclide i (s^{-1})

λ_{ij} is the decay constant of nuclide j producing i (s^{-1})

σ_i is the total cross section for reactions on i (cm^2)

σ_{ij} is the reaction cross section for reactions on j producing i (cm^2)

σ_k^f is the fission cross section for reactions on actinide k (cm^2)

Φ is the neutron flux (n cm^{-2} s^{-1})

S_i is the source of nuclide i from fission

Y_{ik} is the yield of nuclide i from the fission of nuclide k

The final term is only required if actinides are included in the initial material.

FISPACT requires connection to several data libraries before it can be used to calculate inventories. The following libraries are required:

- Cross section data for neutron induced reactions
- Uncertainty data for neutron induced reactions
- Decay data
- Fission yield data
- Biological hazard data
- Legal transport data
- Clearance data
- Gamma absorption data
- Charged particle ranges in materials
- Emitted particle spectral data (from neutron induced reactions)

• Charged particle cross section data

The last three libraries are only required if sequential charged particle effects are included.

The European Activation File (EAF) is the collection of nuclear data that is required to carry out inventory calculations of materials that have been activated following exposure to neutrons. One of the components of EAF is the collection of neutron-induced cross section data. Neutron-induced cross section data must be available in the EAF format (modified ENDF/B-6) in a standard energy group structure. The standard structures are WIMS (69), GAM-II (100), XMAS (172), VITAMIN-J (175) and TRIPOLI (315).

FISPACT uses external libraries of reaction cross sections and decay data for all relevant nuclides to calculate an inventory of nuclides produced as a result of the irradiation of a starting material with a flux of neutrons. The actual output quantities include the amount (number of atoms and grams), the activity (Bq), α-, β- and γ-energies (kW), γ dose-rate (Sv h^{-1}), the potential ingestion and inhalation doses (Sv), the legal transport limit (A value), the clearance index and the half-life for each nuclide. Amounts and heat outputs are also given for the elements and the γ-ray spectrum for the material is listed as well as various summed quantities, such as total activity and total dose-rate. At the end of each time interval the dominant nuclides (in terms of activity, heat, γ dose-rate, potential biological hazards and clearance index) and the pathway data for the production of these nuclides can be shown.

CHAPTER 3

Neutronics assessment of Li/V-alloy and Flibe/V-alloy blankets for FFHR2

3.1 Li/V, Li/Be/V, Flibe/V and Flibe/Be/V blankets

The design of self-cooled molten salt Flibe blanket design for FFHR has been carried out using reduced activation ferritic steel (JLF1) as structure materials [58-59, 61-62]. The thermal efficiency of the plant is relatively low due to high melting point of Flibe (~430 °C) and the limit of maximum operation temperature of JLF1(~550 °C). On the other hand, vanadium alloys (V-alloys) have good thermal-mechanical properties and can be operated up to ~700 °C [33]. So the blanket with the structural materials of V-alloys has potentiality for higher thermal efficiency. For blankets using V-alloys, liquid Li and Flibe were proposed as candidate liquid tritium breeders [63,64]. Liquid Li is an attractive breeding material due to high Li content, high thermal conductivity and good compatibility with V-alloys to high temperature. But the flow of Li in magnetic field would cause an issue of MHD pressure drop. The application of MHD insulator coating, e.g. Er_2O_3 [65-66], is necessary for Li blanket.

Flibe posses several attractive features such as low electric conductivity and low reactivity with water and air [59]. The deposition of WF_6 or MoF_6 into Flibe was proposed to reduce corrosive TF produced as the result of transmutation of Flibe and to plate the wall with anticorrosive W or Mo [64,67].

Be is a potentially necessary neutron multiplier. Be is also an excellent neutron moderator with low absorption cross section for thermal neutrons. Use of Be is an option for both Li and Flibe blankets for FFHR2m although there are some issues specific to Be such as resource limitation and

irradiation effect.

Four blankets concepts using Li or Flibe as tritium breeder and coolant with V-alloy structure were proposed for FFHR2m design as following:

- Self-cooled flibe with V-alloy structure (Flibe/V)
- Self-cooled flibe with Be multiplier and V-alloy structure (Flibe/Be/V)
- Self-cooled Li with V-alloy structure (Li/V)
- Self-cooled Li with Be multiplier and V-alloy structure (Li/Be/V)

Two self-cooled blankets concepts, Li/V and Flibe/V were investigated for FFHR2m such as assessment of tritium breeding ratio (TBR) and shielding of Li/V and Flibe/V [67,68]. Some neutronics issues such as blanket energy multiplication and neutron activation need to be assessed for Li/V and Flibe/V blankets. Flibe/Be/V and Li/Be/V blankets are also proposed for FFHR2m design. Because of the neutron spectral difference, the neutronics issues may be different for the Li/Be/V and Li/V and for the Flibe/V and Flibe/Be/V blankets.

The objectives of the present study are to assess impact of the external Be on the tritium breeding and shielding performance of Li and Flibe blankets for FFHR2m design, and to investigate the activation issues such as the activation of MHD coating of Er_2O_3 and Flibe.

3.2 Neutronics assessment of Li/V-alloy and Flibe/V-alloy blankets for FFHR2

3.2.1 Design requirements and FFHR2m1 design windows

Here, the design window and the neutronics design requirements of FFHR2m1 are reviewed with respect to tritium breeding, shielding for magnet and nuclear energy deposition.

Attaining tritium self-sufficiency is necessary for the D-T fueled fusion reactors. Tritium is bred in blankets though the reactions with lithium. To achieve the tritium self-sustaining, a required TBR for a reactor should account for the tritium to be burned in the plasma, lost by decay and also necessary for supplying inventory for the startup of other plants. The required TBR largely depends on tritium storage inventory and doubling time, etc. The calculated achievable TBR should greater than the required TBR with enough margins considering the uncertainties in estimations of tritium production and transport [76,77]. It was reported that the achievable TBR of only ~ 1.01 would be necessary without considering uncertainties [78]. Considering the inherent uncertainties in the transport calculation due to the uncertainties in the physics data, calculation method, and modeling, it was required that the calculated TBR is to be greater than 1.10 [79].

The investigations of the effective space for tritium breeding in FFHR have been carried out [61,75]. It was seen that the effective blanket coverage for FFHR2m1 is ~80% based on detailed 3-D description of helical structures [75]. Efforts to increase the blanket coverage fraction have been continued in the reactor design activity. An effective coverage of 85% is adopted in the

present study. Therefore, the requirement on the calculated local TBR, assuming a simple torus model with 100% blanket coverage, was defined to be ~1.30 to achieve tritium self-sufficiency.

In a fusion reactor, the function of a superconducting magnet can be influenced during the reactor operation through radiation damage to the magnet components. The shielding region following breeding region is designed to protect the superconducting magnet. The radiation limit for superconductor magnet determines the thickness of shielding.

In the superconductors, the possible influences of radiation are by neutrons and photons resulting in the change of damage of the critical temperature, Tc, and the critical current, Jc of the superconducting material, loss of mechanical property of the insulting and structural material [80-82]. Recent estimate showed that the change of Tc and Jc induced by neutron bombardment will be the limiting factor. For Nb_3Sn, it was reported that end-of life fast neutron fluences up to 10^{19} n/cm^2 ($E > 0.1\ MeV$) will not result in significant degradation in superconducting property [82].

One of the basic functions of the blanket is to convert their kinetic energy into heat. The blanket energy multiplication (M) is given by the ratio of the heat deposited in the blanket to the source neutron kinetic energy, i.e.

$$M = \frac{\text{Blanket heat deposition (MeV per D-T neutron)}}{14.1\ \text{MeV}}$$

In order to obtain a higher thermal power output, the blanket energy multiplication is to be as large as possible. The heat deposited in the cold

shield should be designed to be as small as possible because it will not be recoverable.

In this study, flibe and Li blankets are proposed for FFHR2m1 design. The space for blanket is limited in FFHR2m1. Maximum thickness for blanket including shielding is 1.2 m. The design requires detailed neutronics examinations. Key design goals for FFHR2m are: an overall tritium breeding ratio (TBR) of ~1.1 (local ~1.3) and fast neutron fluence (>0.1 MeV) at superconducting magnet with 30 years operation is less than 10^{19} n/cm^2. Table 3.1 lists the design parameters, required TBR and radiation limits for FFHR2m1 design.

Table 3.1 Design parameters, tritium breeding requirement and radiation limits

Fusion power	1.9 GW
Major radius	14.0 m
Minor radius	1.73 m
Blanket space	1.2 m
Neutron wall loading	1.5 MW/m^2
Machine lifetime	30 years
Overall TBR	~1.1
Local TBR	~1.3
Fast neutron fluence (E>0.1MeV) at magnet for the lifetime	10^{19} n/cm^2

3.2.2 Calculational procedure

A simple torus model of FFHR2 [68] was used in neutronics calculation. The plasma major and minor radius of the present modified FFHR2 design, FFHR2m1 [62], is 14 and 1.73 m, respectively. The average neutron wall loading is 1.5 MW/m^2. The available space for the blanket is 120 cm. The schematic radial distributions of the Li/Be/V and Flibe/Be/V blankets are shown in Fig. 3.1. V-alloy of 5 mm in thickness was employed as the first wall. Tungsten armor was attached on the surface with thickness of 5 mm. The mixture of 70% JLF-1 and 30% B_4C was chosen for radiation shielding as designed for the Li/V and Flibe/V blankets [68]. The Li or Flibe coolant was separated by V-alloy walls. The cooling channels in the shielding region are neglected for the calculation. The solid Be was used in the Li/Be/V and Flibe/Be/V blankets for multiplying neutrons. A 5 cm Be zone in pebble form (65% Be+35% Flibe+5% V-alloy) or layer (90% Be+10% V-alloy) was applied in the Flibe/Be/V or Li/Be/V blanket. The Be zones were arranged 6 cm from FW as shown in Fig. 3.1. The achievable TBR with 35% of ^{6}Li enrichment is near the maximum for Li/V and Flibe/V blankets [68]. The ^{6}Li enrichments for Flibe/Be/V and Li/Be/V blankets were fixed to 35% to show the impact of Be on the TBR in this study. For the Li/V and Li/Be/V blankets, the electrical insulator coating of Er_2O_3 with thickness of $\sim$10 μm was assumed in the interface between Li and V-alloy walls to reduce the induced MHD pressure drops by the flows of Li in high magnetic fields.

The neutronics analyses for the breeding blankets of FFHR2 were

performed with MCNP-4C code [70] and JENDL-3.2 file [83].

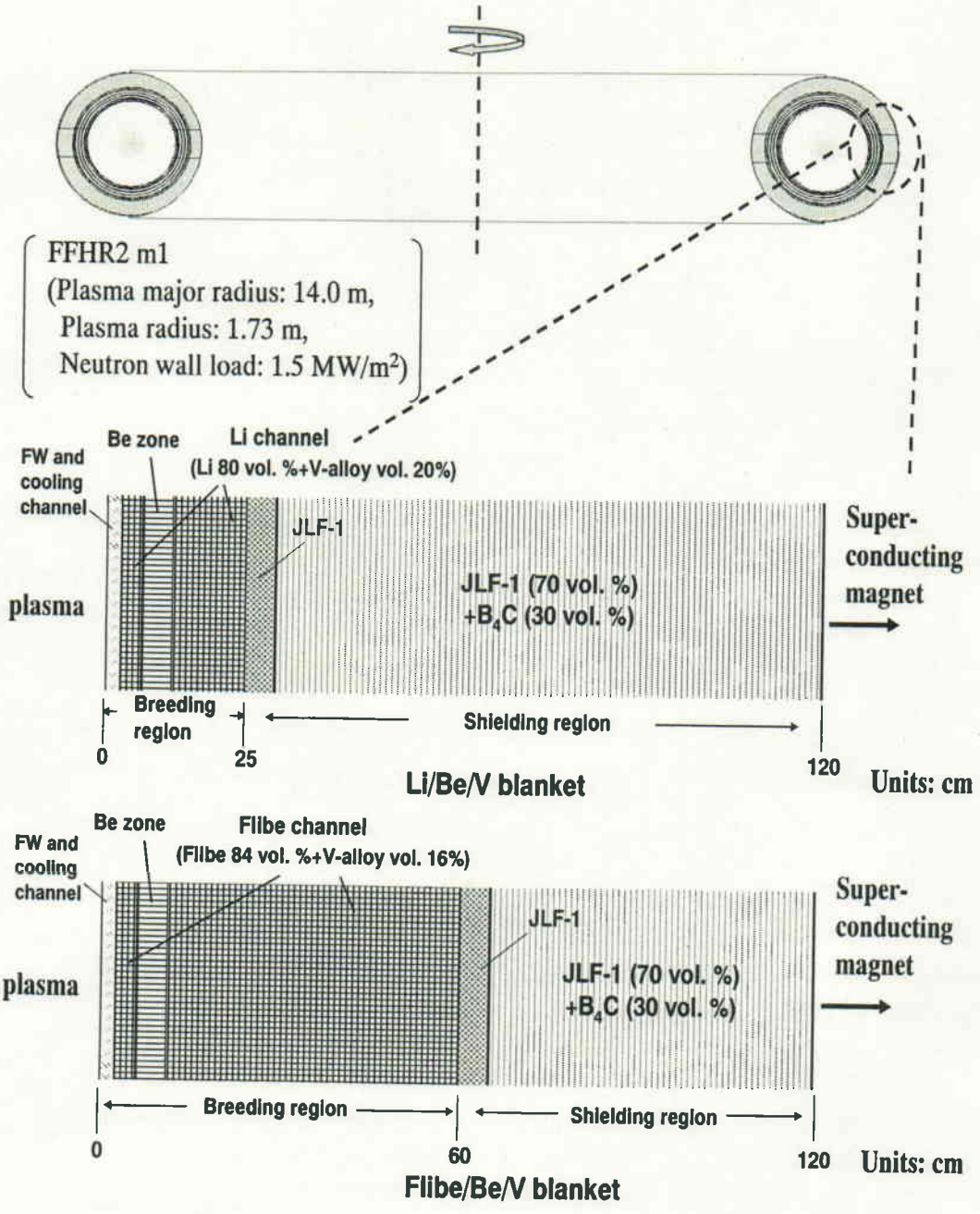

Fig.3.1 Schematic radial distribution of the Li/Be/V and Flibe/Be/V blankets

3.2.3 Tritium breeding and shielding performance

The comparison of the typical neutron spectra in liquid blankets with and without Be was shown in Fig.3.2. All spectra were chosen at the position of 19.5 cm from FW. Beryllium effectively multiplies neutrons through the (n, 2n) reaction. In addition, Be also is an excellent neutron moderator with much lower absorption cross section for thermal neutrons compared to Li. Beryllium increased low energy neutrons significantly, especially for the Li/Be/V blanket. Thus, tritium breeding through ^{6}Li(n, t) reaction is enhanced. Some calculation results of Li/Be/V and Flibe/Be/V were compared with Li/V and Flibe/V in Table 3.2. The neutronics analysis for Li/V in [68] show that the necessary thickness of the breeding region for obtaining adequate TBR in Li/V is ~55 cm. It is possible for Li/Be/V to obtain the same TBR with thinner breeding region compared to Li/V due to the high neutron multiplication capability of Be. The TBR of 1.35 can be achieved in Li/Be/V with a 25 cm breeding region. Because of the resulting increase in the shield thickness, the shielding property of Li/Be/V is improved significantly. The fast neutron flux (>0.1 MeV) at outside of radiation shield in the Li/Be/V blanket is 4.9×10^{8} n/cm^{2}/s, ~5.6 % of that in the Li/V blanket. However it should be noted that the heat removal from the breeding zone of 25 cm is not feasible. Optimization of the thickness is necessary for tritium breeding and heat control purpose.

With the same thickness of breeding region, the TBR of the Flibe/Be/V blanket is remarkably higher than that of the Flibe/V blanket. However the

shielding performance of the Flibe/Be/V blanket is almost the same as that of the Flibe/V blanket..

There are small changes (< 0.1%) of TBR for Li/V and Li/Be/V blankets with Er_2O_3 coating in 1-10 μm. The effect of Er_2O_3 coating on the TBR is neglected.

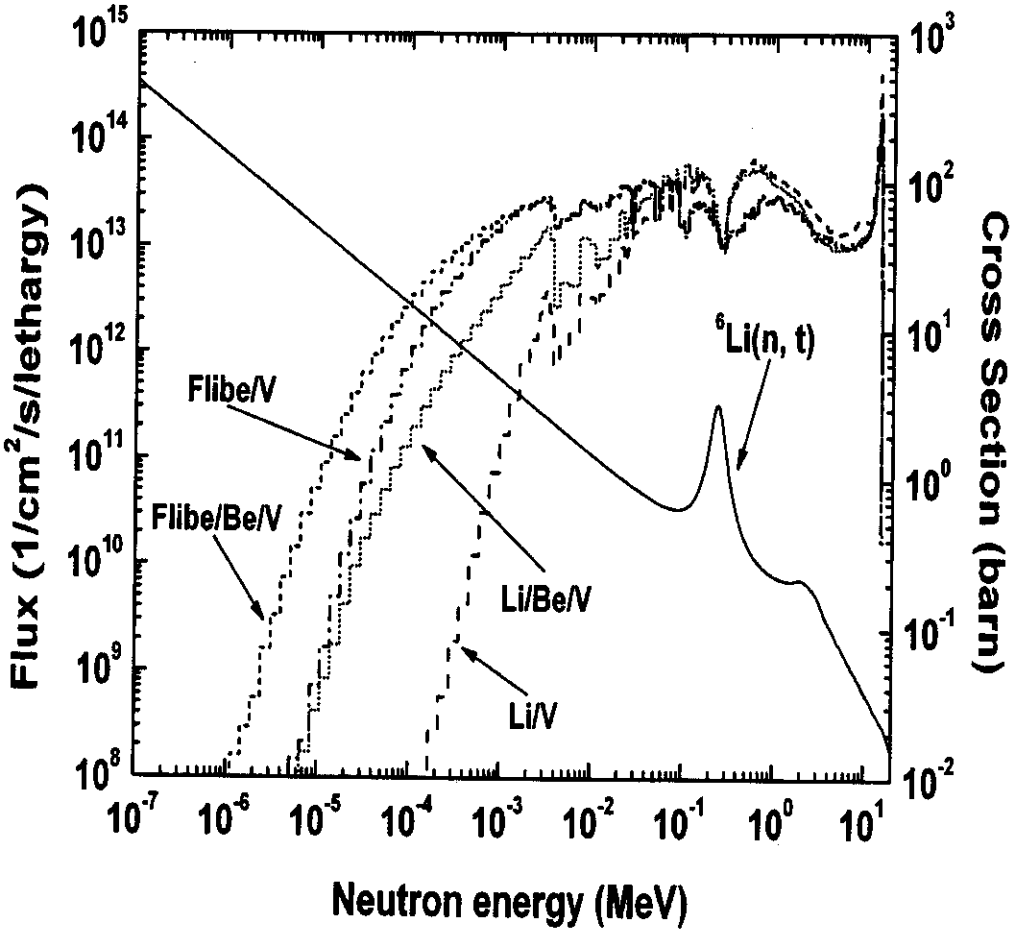

Fig.3.2 Typical neutron spectra of liquid blankets and the $^6Li(n,t)$ cross section.

Considering 30 years operation for magnet, the end-of-life fast neutron

fluences (E> 0.1MeV) in the magnet for Li/V, Li/Be/V, F/V, and F/Be/V blankets are 8.2×10^{18}, 1.0×10^{18}, 1.3×10^{18}, and 1.2×10^{18} n/cm^2, respectively, which are below the proposed limits of 10^{19} n/cm^2 for Nb_3Sn [82].

Table 3.2 Comparison of neutronics calculation for liquid blanket systems

Blanket type	Li/V	Li/Be/V	Flibe/V	Flibe/Be/V
Solid neutron multiplier	none	Be	none	Be
MHD coating	Er_2O_3	Er_2O_3	none	none
Enrichment of ^{6}Li(%)	35	35	35	35
Thickness of breeding region	54	25	60	60
Thickness of shielding region	66	95	60	60
Local TBR	1.34	1.35	1.26	1.40
Fast neutron flux(>0.1MeV) at outside of radiation shield (10^9 n/cm^2/s)	8.7	0.49	1.4	1.3
Fast neutron fluence(>0.1 MeV) after 30 years' operation at outside of radiation shield (10^{18} n/cm^2)	8.2	0.46	1.3	1.2

3.2.4 Nuclear heating

The nuclear heating deposition and energy multiplication for four blankets are summarized in Table 3.3. The Li/Be/V blanket produces the highest energy multiplication of 1.24. The deposited energy from gamma are ~25%, ~31%, ~28% and ~26% of the total energy in Li/V, Li/Be/V, Flibe/V and Flibe/Be/V blankets, respectively. For Flibe/V and Flibe/Be/V, more than 99% energy is deposited in breeding region. However, 6.6% and 11% energy are leaked into the shielding in Li/V and Li/Be/V, respectively. The energy deposited in cold shielding region is less efficient for power generation. It may be necessary to design the shielding region as separated into the high temperature (HT) and the low temperature (LT) regions for Li/V and Li/Be/V blankets. The energy recovered in the HT shielding region may need to be used to enhance the economy of the reactor.

Table 3.3 Energy deposition and energy multiplication for four blankets systems

Energy deposition	Li/V		Li/Be/V		Flibe/V		Flibe/Be/V	
	Breeding region	Shielding region	Breeding region	Shielding region	Breeding region	Shielding region	Breeding region	Shielding region
neutron	11.8 MeV	0.4 MeV	11.3 MeV	0.81 MeV	11.6 MeV	0.04 MeV	12.4 MeV	0.04 MeV
gamma	3.5 MeV	0.7 MeV	2.99 MeV	2.33 MeV	4.40 MeV	0.08 MeV	4.32 MeV	0.09 MeV
Total	16.4 MeV		17.4 MeV		16.1 MeV		16.8 MeV	
M	1.16		1.24		1.14		1.19	

3.3 Activation of Li/V-alloy and Flibe/V-alloy

3.3.1 Calculational procedure

The activation of four blankets proposed in FFHR2m1 design was investigated. Figure 3.3 shows the activation analysis procedure. The neutron flux used in activation calculation was calculated by MCNP-4C code and JENDL-3.2 library. The average neutron loading is 1.5 MW/m^2. The calculation model of the blanket structure is shown in Fig 3.1-2. The activation analysis was performed using FISPACT-2001 code with EAF-2001 files [72,73]. The activation cross section in 175 group structure was used in the calculation. For limited cases, the continuous cross section of JENDL-3.3 combined with MCNP-4C was utilized to show the grouping effect on the activation calculation [84].

The plant is designed to operate for 30 full power years. Potential replacement of the blankets is considered whose frequency mostly depends on the lifetime of structural materials and Be if any. Thus, in this case, the time of 10 full power years was assumed in activation analysis of blankets including shielding. The MHD coating of Er_2O_3 was considered in the calculation.

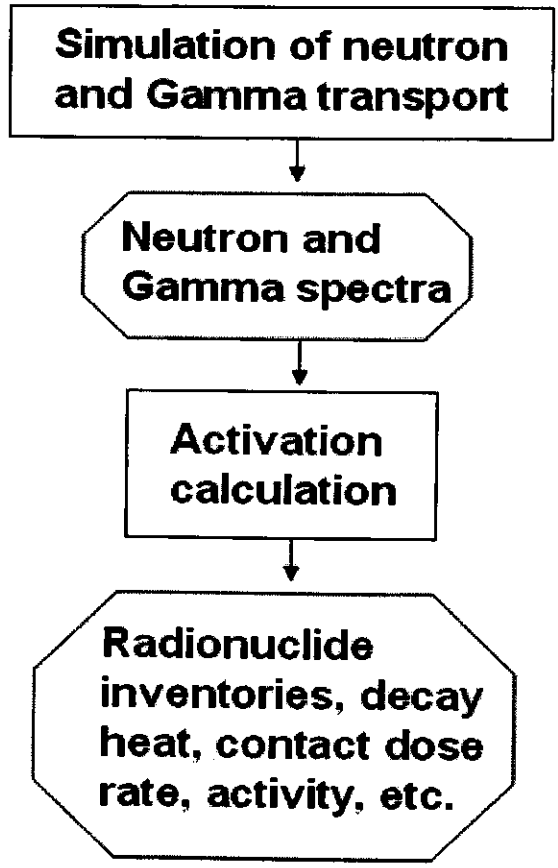

Fig.3.3 Procedure of analysis of the activation of liquid blanket system

3.3.2 Activation analysis

[I] Effect of the activation of Er_2O_3 coating in the Li/V and Li/Be/V blankets

In this study, the effect of the activation of Er_2O_3 coating was analyzed. Figure 3.4 shows the comparison of dose rate of the structural component with and without coating for the Li/V and Li/Be/V cases. In the figure, the recycling criteria of Remote (Dose rate < 10 mSv/h) and Hands-on recycling (Dose rate < 10 μSv/h) are indicated [85]. For the case with Er_2O_3 coating the

dominant nuclide is ^{166m}Ho ($T_{1/2}$, 1200 yr) in the range from several tens to thousand years. ^{166m}Ho is the activation product of Er_2O_3 coating. There are three activation paths for ^{166m}Ho, namely ^{166}Er(n, p) ^{166m}Ho, ^{164}Er (n, γ)^{165}Er (EC)^{165}Ho(n, γ)^{166m}Ho and ^{166}Er(n,2n)^{165}Er(EC)^{165}Ho(n, γ)^{166m}Ho. It is shown in Fig. 3.4 that the production of ^{166m}Ho in the Li/Be/V blanket is about twice that in the Li/V blanket because of the enhancement of the reactions of ^{164}Er (n, γ) ^{165}Er and ^{165}Ho (n, γ) ^{166m}Ho with low energy neutrons in the Li/Be/V blankets.

It is shown that V-alloy is a good low activation material and can be recycled by hands-on operation after ~20 years' cooling, while V-alloy with the coating needs shielding for recycling even after 1000 years cooling. However, recycling is still feasible with 10 μ m-thick Er_2O_3 coating. Activation with 1 μ m is much lower and approaches Hand-on Recycling Limit. Higher cost for the recycling of V-alloy structural materials with Er_2O_3 coating would be needed than that of the bare V-alloy, especially in the case of using external solid Be.

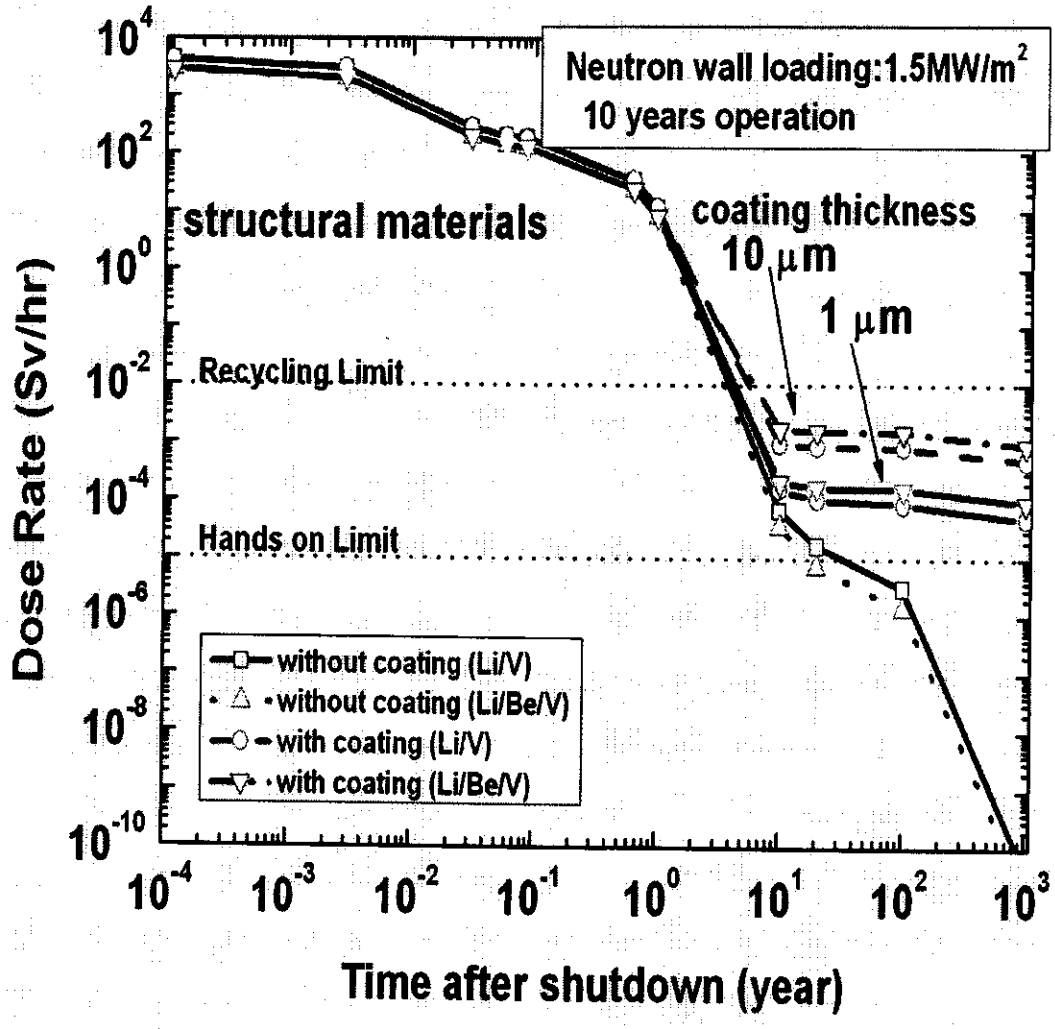

Fig.3.4 Dose rate of structural component with and without Er_2O_3 coating.

[II] Activation of Flibe/V and Flibe/Be/V blankets

The decays of the dose rate of V-alloy and Flibe vs. cooling time in the Flibe/V and Flibe/Be/V blankets are plotted in Fig. 3.5. The activation of the Flibe/Be/V blanket is comparable to that of the Flibe/V blanket. After 10

years operation, V-alloy could meet the hands-on requirement at the cooling time of several tens years. Flibe is re-circulated along the coolant channel inside and outside the blankets at the operation time. Here 10 days continuous irradiation was assumed for the activation analysis of Flibe as a simplification of the periodical irradiation and cooling in and out of the blanket, respectively. Flibe could decay to negligible level sooner compared to structure materials of V-alloy. The dominant radionuclide in Flibe is ^{18}F ($T_{1/2}$, 1.83 hr) produced by $^{19}F(n, 2n)^{18}F$ reaction with high threshold energy. Flibe has slightly lower induced dose rate in the Flibe/Be/V than that in the Flibe/V due to the lower neutron flux at high energy.

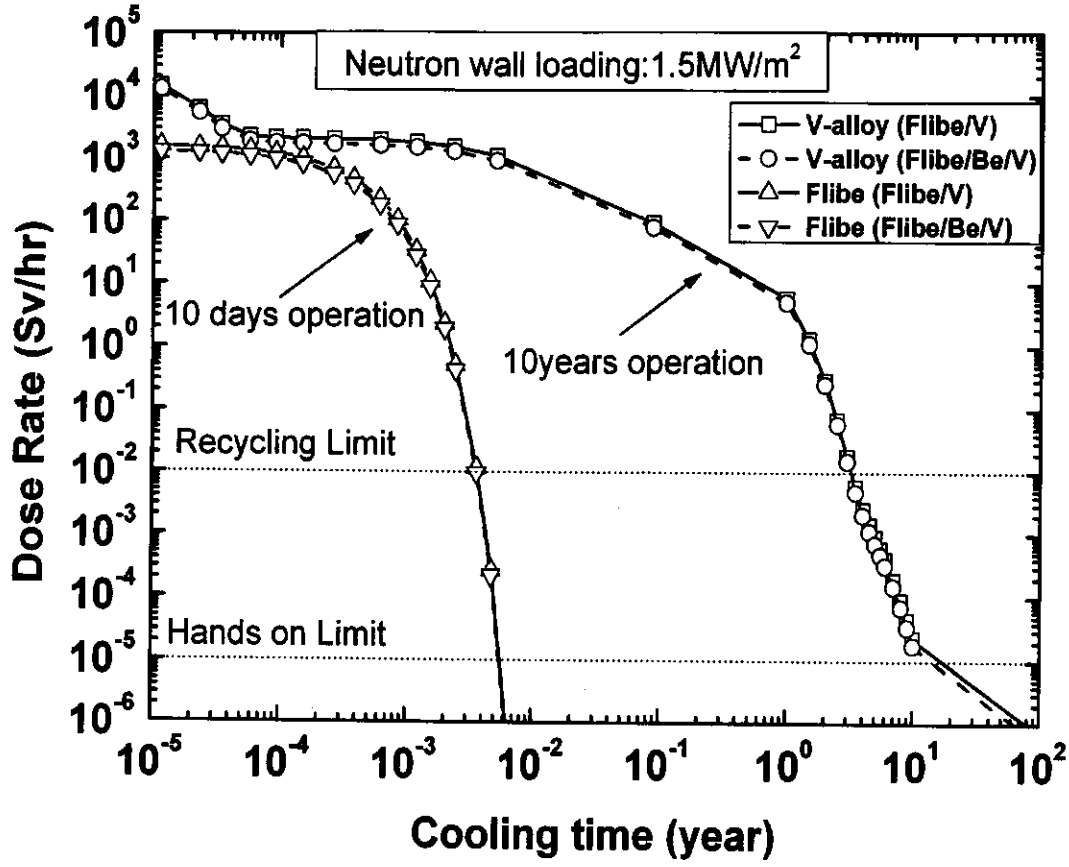

Fig.3.5 Dose rate of Flibe with 10 days operation and V-alloy with 10 years operation vs. cooling time.

3.3.3 Remaining issues

The accurate estimate the activity of dominant radioactive nuclide is necessary. For Li blankets, ^{166m}Ho is one of the key radioactive nuclides. The important activation reactions of ^{164}Er (n, γ)^{165}Er for the product of ^{166m}Ho have high cross section at thermal neutron region and huge resonance peaks. The cross section of continuous cross section from JENDL-3.3 was used for ^{164}Er(n, γ)^{165}Er to check the grouping effects in activation calculation. Increase of dose rate in 20% by using continuous cross section for ^{164}Er(n, γ)^{165}Er was derived as shown in Fig. 3.6. Thus, a guideline for using the

activation cross section data is necessary. The codes and data applied for activation analysis need to be verified by comparison between calculation and experiment. This is motivating the study of Chapter 4.

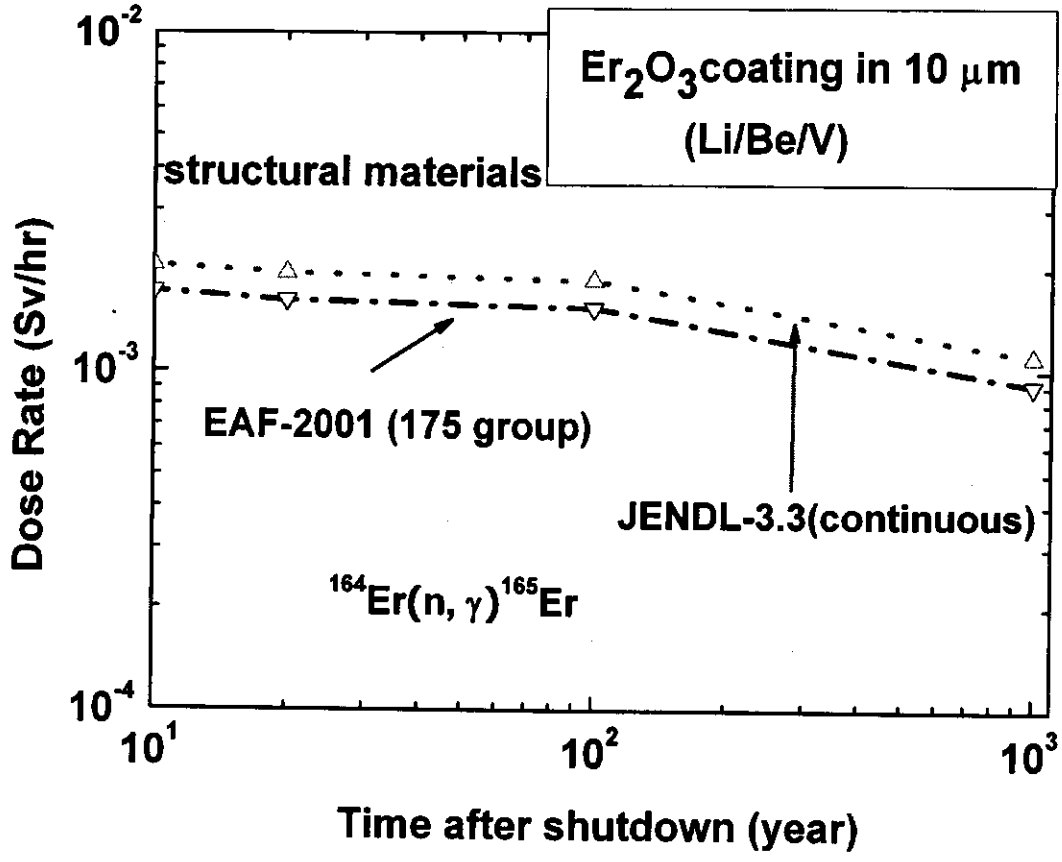

Fig. 3.6 Grouping effect of ^{164}Er (n, γ)^{165}Er

3.4 Summary

The neutronics assessment for the impact of the external Be on the tritium breeding, shielding performance and activation of Li and Flibe blankets for FFHR2m design were performed. Conclusions on suggestion to FFHR2m blanket design are

I. Advantage of the use of Be is quantified. With Be, TBR design margin for Li and Flibe blankes could be improved. For Li blanket with Be, the shielding design margin could also be improved with adequate TBR. The results provide information necessary for characterizing trade-off of using Be in Li and Flibe blankets.

II. Recycle of structural materials is still feasible with Er_2O_3 coating in 10 μm, and with 1 μm thickness the activation is reduced and approaches Hands-on Recycling Limit. Thinner Er_2O_3 coating is recommended from neutronics performance.

III. The dominant activation product in Flibe is ^{18}F ($T_{1/2}$, 1.83 hr), potentially causing short-term hazard in maintenance and release event

IV. The use of continuous cross section can increase the activation of Er by 20%

→ A guideline for using the activation cross section data is necessary.

CHAPTER 4

Activation experiment on the materials relevant to Li/V and Flibe/V blankets

4.1 Introduction

Li/V-alloy and Flibe/V-alloy are proposed for FFHR2 blanket design. The induced radioactivity in liquid blankets is recognized as one of the most critical issues from a safety viewpoint. Safety studies for liquid blankets of FFHR2 were performed by computer tools (codes and data) in Section 3.3. Significant difference for the prediction of the activation product of ^{166m}Ho was observed between the cases with grouped and continuous activation cross section data. Accurate predictions of radioactivity are important in safety design of fusion reactors. Thus, it is essential to verify the calculation codes and associated data.

Major aim of this study is to verify or improve the procedure for calculating activation which can be applied to liquid blankets, by comparing radioactivity derived by calculation and experiment. A series of irradiation experiments were performed using Fusion Neutronics Source (FNS) at JAEA with the purpose of evaluating neutron activation of materials relevant to Lithium/V-alloy and Flibe/V-alloy blankets. Be, Li and Li/Be mock-ups were assembled with Be and solid Li blocks in addition to the assembly for direct D-T neutron irradiation to examine the dependence of the activation on neutron spectrum.

This is unique effort to investigate the activities of liquid breeder relevant materials induced in neutron fields simulating the prototypical fusion neutron spectra in various blankets.

4.2 Experiment and analysis

The comparison of the candidate neutron sources for fusion neutronics study is shown in Table 4.1 [86,87]. FNS is the most suitable means for neutronics study except for those requiring higher neutron fluxes.

The irradiation experiments were performed using the 80° beam line of FNS at JAEA. Figure 4.1 shows the Bird's Eye View of FNS facility. 14 MeV neutrons were generated from D-T reactions by the impingement of a 2mA deuteron beam of 350 keV on a stationary tritium-bearing target ($TiT_{1.7}$) cooled by water. Nominal neutron yield at the target was $3x10^{11}$ n/s. The neutron irradiation history was recorded with multichannel scaling (MCS) per 10 s.

Three materials relevant to Lithium/vanadium-alloy and Flibe/vanadium-alloy blankets, NIFS-HEAT-2, Er and Teflon (CF_2), were used in the experiment. Er specimens are the pure metallic foils in 99.9%. NIFS-HEAT-2 is an alloy of V-4Cr-4Ti. The specimens of NIFS-HEAT-2, Er and Teflon in 10 mm×10 mm×0.03-0.1 mm were prepared for studying the activation of V-alloy structure, Er in MHD coating of Er_2O_3, and F in molten salt Flibe, respectively. Masses of specimens are in the range of 30-100 mg. The specimens are shown in Fig. 4.2.

The irradiation experiments were performed with pure D-T neutrons and with moderated neutrons in Be, Li, and Be/Li mock-ups. The direct D-T neutron irradiation was conducted using a pneumatic tube to send specimens to the position 15 mm from the tritium-titanium target. Thin Nb

foils with 10 mm×10 mm×0.05 mm were attached to the specimens to monitor 14 MeV neutrons fluence.

Table 4.1 Comparison of neutron source characteristics.

	Flux	Spectra	Use for irradiation	Accessibility	comments
Fission reactors	High	Fission spectra	Well established	Poor	Not very fusion relevant
Spallation neutron sources	Medium	Spallation spectra (wide)	Still limited	Medium	Different from fusion spectra; uncertainties of data (En ≥ 20 MeV)
IFMIF (D-Li neutrons)	High	D-Li neutron spectra (Near D-T)	Not available now	Good	Suitable for fusion materials study

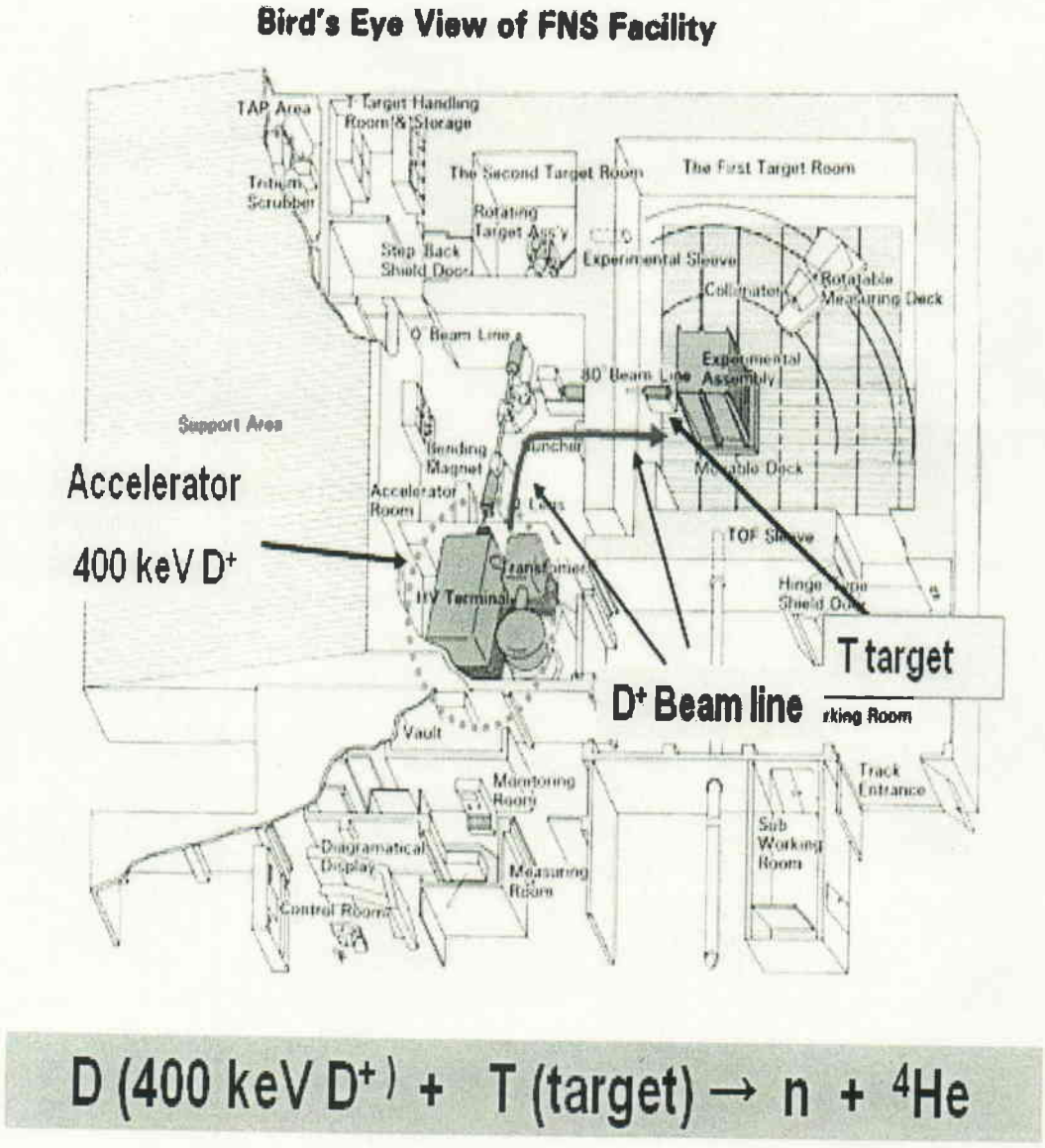

Fig.4.1 Bird's Eye View of FNS facility

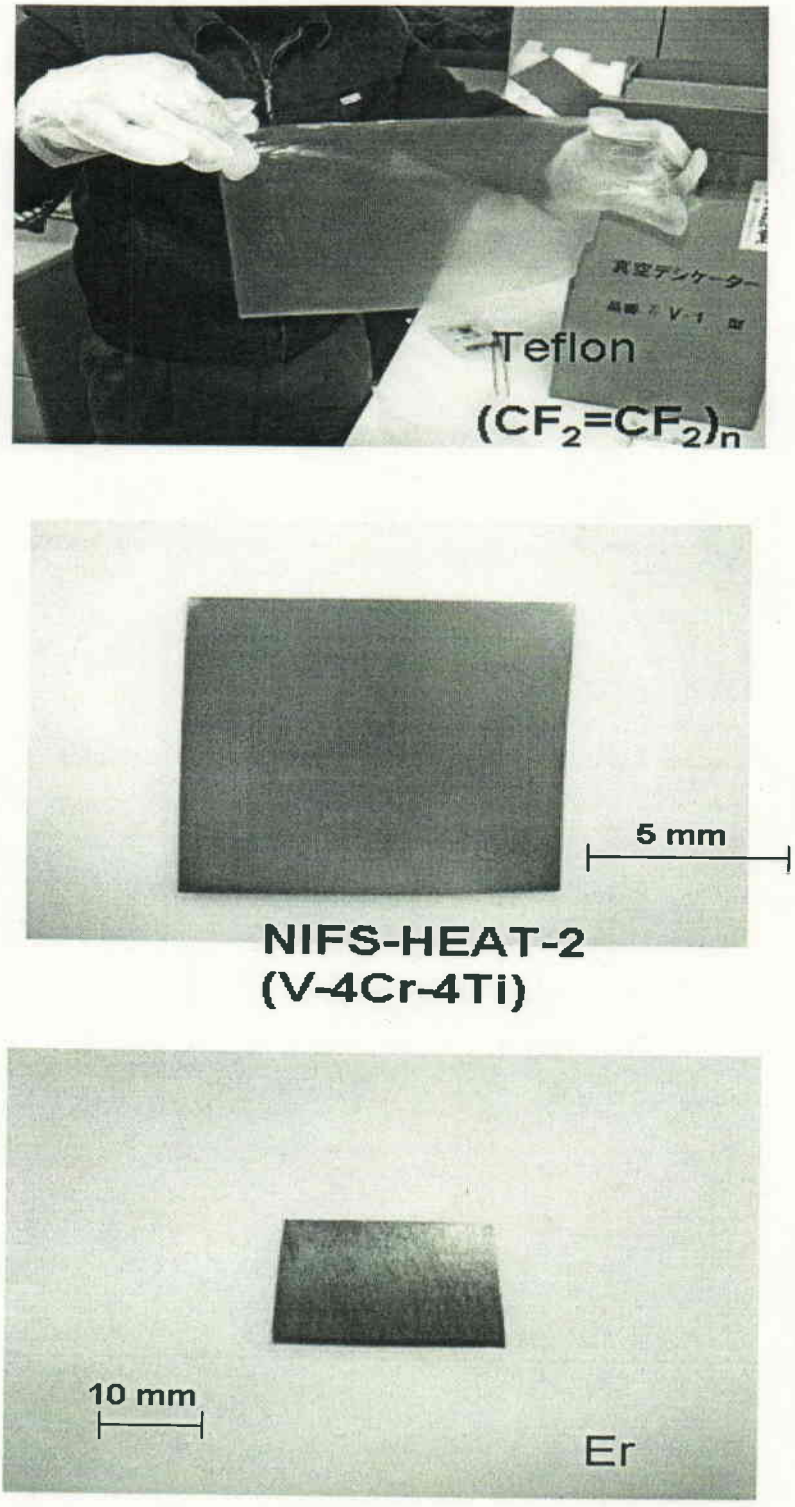

Fig.4.2 The specimens of Teflon and NIFS-HEAT-2 and Er

Be, Li and Li/Be mock-ups of 253 mm×253 mm×306 mm were built with Be and Li blocks. The mock-ups were located ~10 mm from the target. The axis of the central zone was aligned to the d^+ beam direction in order to keep good symmetric configuration. The blocks in 50.6 mm×50.6 mm×50.6 mm were used in the centre zone of mock-ups. The specimens were directly attached to the first and second blocks. The thin Nb foils with 10 mm×10 mm×0.05 mm were attached to the specimens to monitor the fast neutron fluence.

Table 4. 2 Irradiation cases.

Case	*Location*
Case Ⅰ: D-T	D-T (15 mm from target)
Case Ⅱ: Be mock-up	Position A, B (next to the first and second blocks)
Case Ⅲ: Li mock-up	Position A, B (next to the first and second blocks)
Case Ⅳ: Be/Li mock-up	Position A, B (next to the first and second blocks)

All the irradiation cases are listed in Table 4.2. Schematic views of all cases and the locations of the specimens are shown in Fig. 4.3-6.

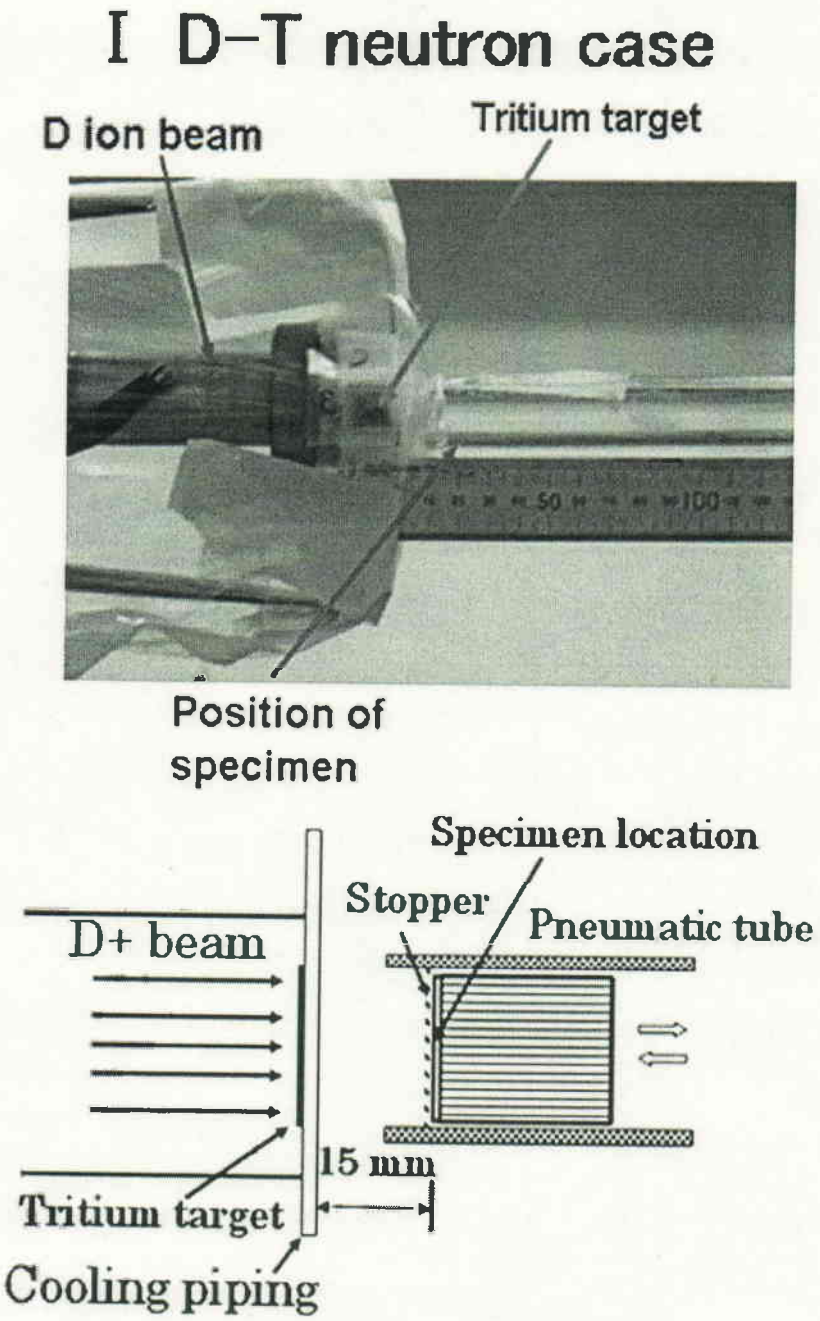

Fig. 4.3 The schematic view of irradiation assembly with D-T neutron.

Ⅱ Be mock-up case

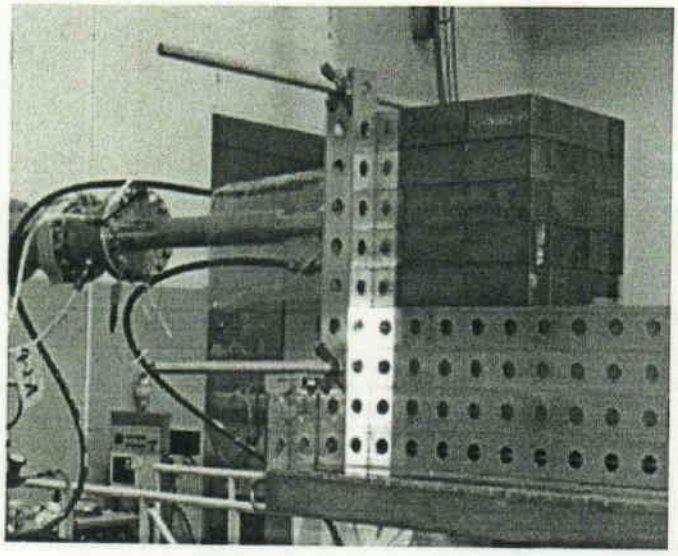

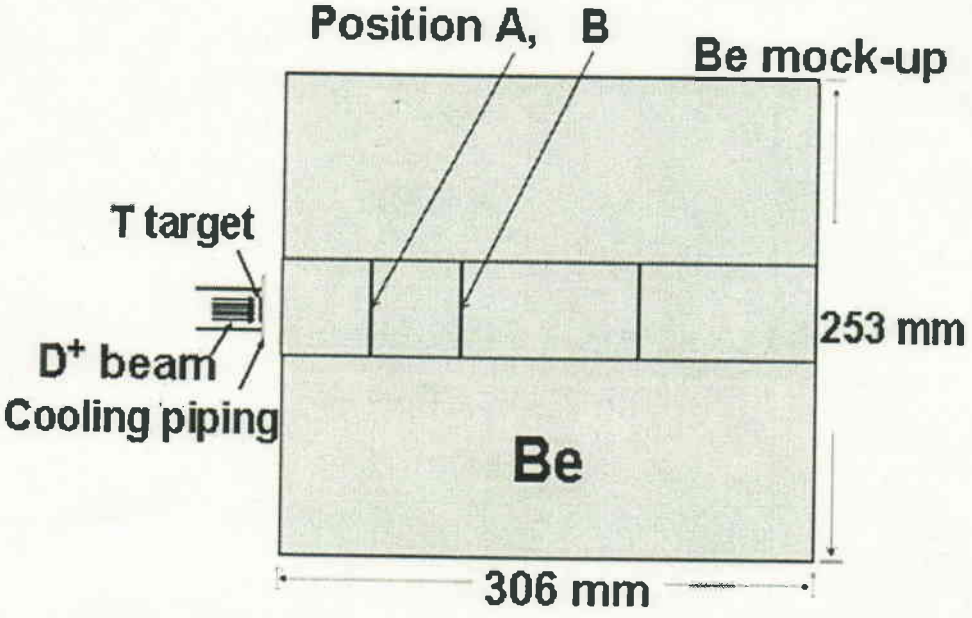

Fig. 4.4 The schematic view of the Be mock-up and irradiation locations

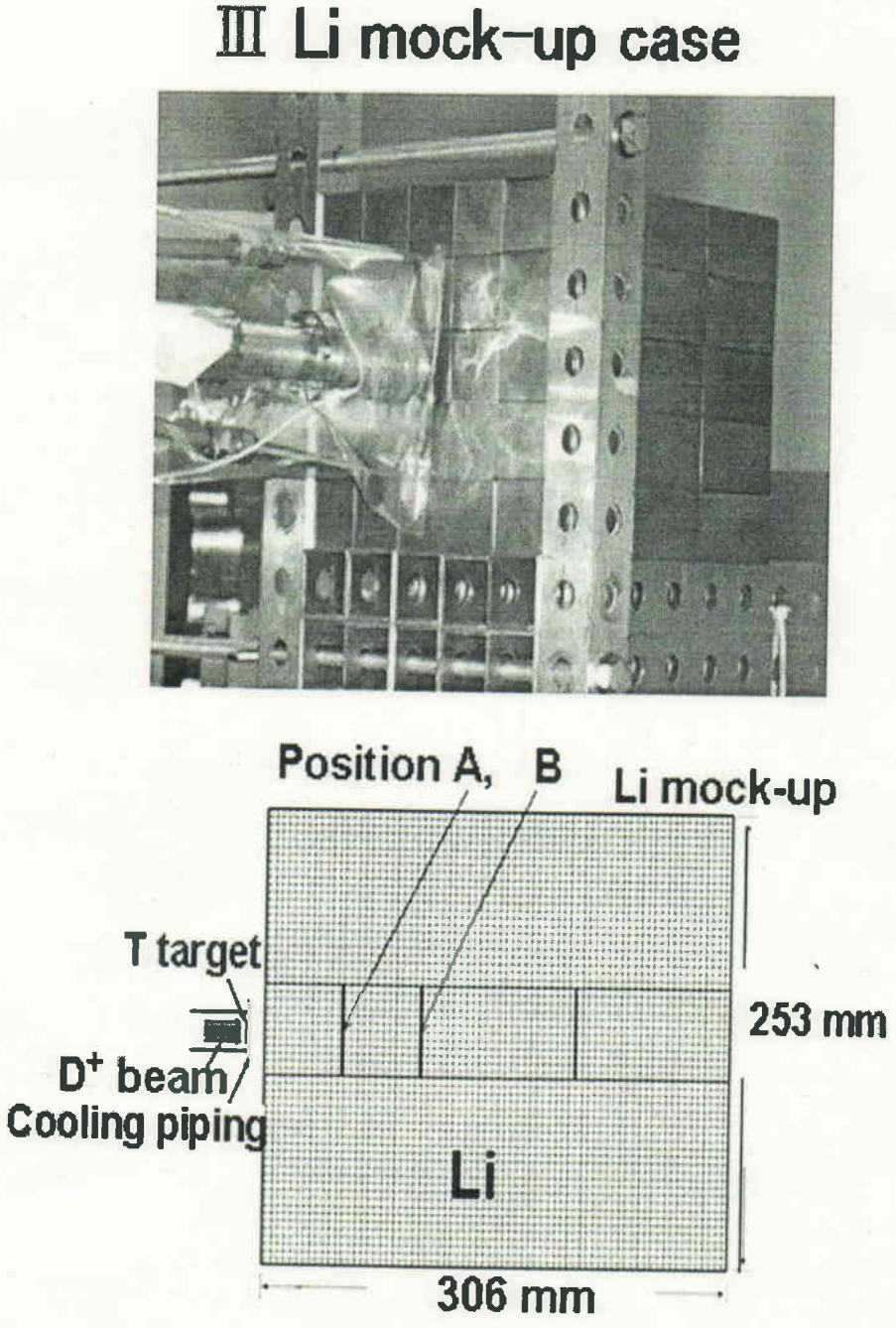

Fig. 4.5 The schematic view of the Li mock-up and irradiation locations

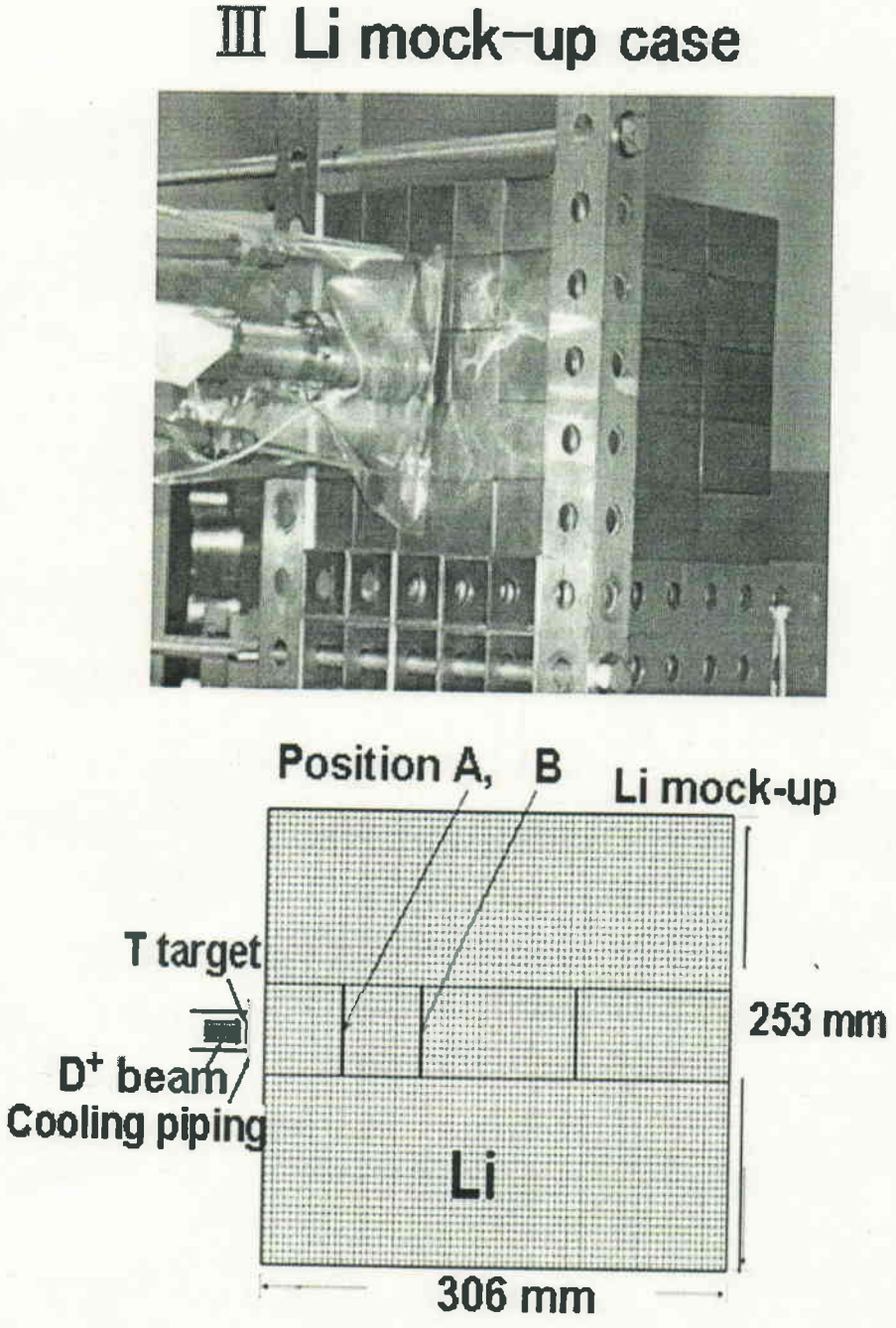

Fig. 4.5 The schematic view of the Li mock-up and irradiation locations

Ⅳ Be/Li mock-up case

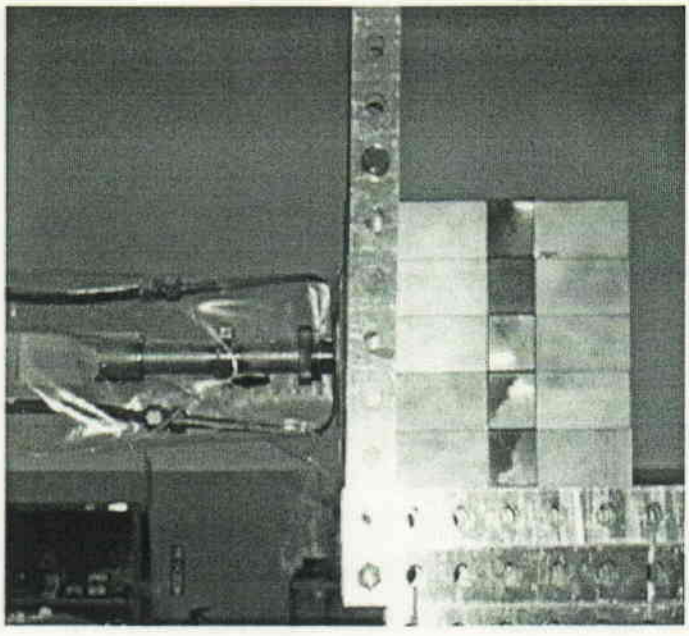

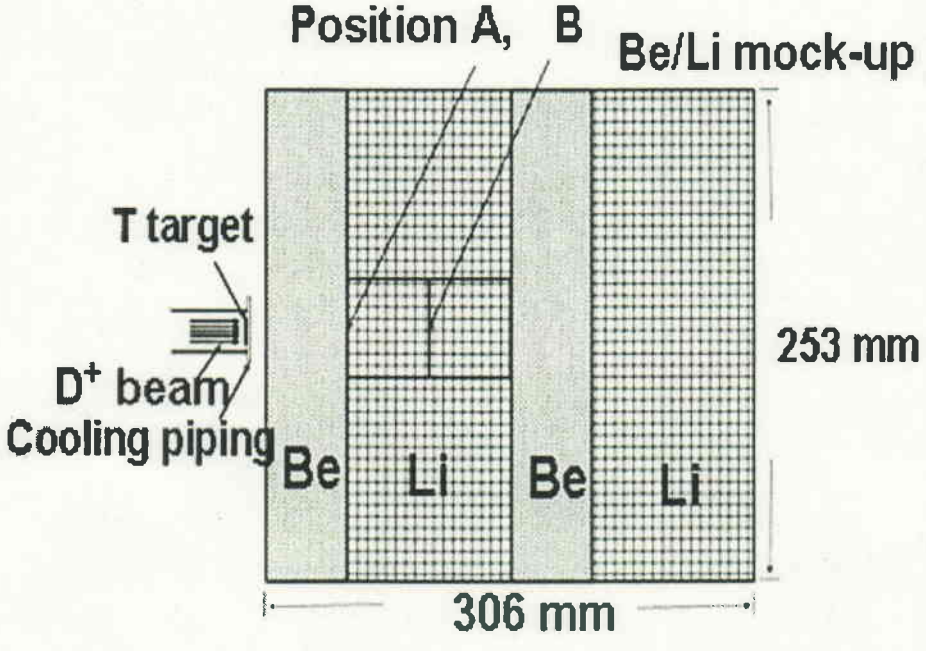

Fig. 4. 6 The schematic view of the Be/Li mock-up and irradiation locations

The irradiation time ranged from 6 minutes to 5 hours depending on the nuclides investigated. After irradiation the gamma-rays emitted from the irradiated specimens were measured with high purity Ge detectors. The activities of radionuclide were obtained from the counts of gamma-rays through the following equation.

$$A(t) = \frac{\lambda S}{I_\gamma \varepsilon (e^{\lambda t_m} - 1)} \qquad (4.1)$$

Where

$A(t)$ is the activity at time t,

S is the counts of peak,

λ is the decay constant,

t_c is the cooling time,

t_m is elapsed measurement time,

t is the sum of t_c and t_m,

I_γ is probability of γemitted,

ε is efficiency of detector.

When there are multiple γ-rays associated with a particular radionuclide, the most intense γ-ray line was used for the data processing.

Figure 4.7 is an example of measured gamma spectra of the irradiated specimen of Er in Be mock-up case. Unique gamma ray of 308.3 keV with a 66.0 % probability was released in the decay process of ^{171}Er. The activity of ^{171}Er can be derived through equation 4.1. The activity of ^{171}Er as a function

of time is determined by the gamma ray counts measured at different cooling times as shown in Fig. 4.8.

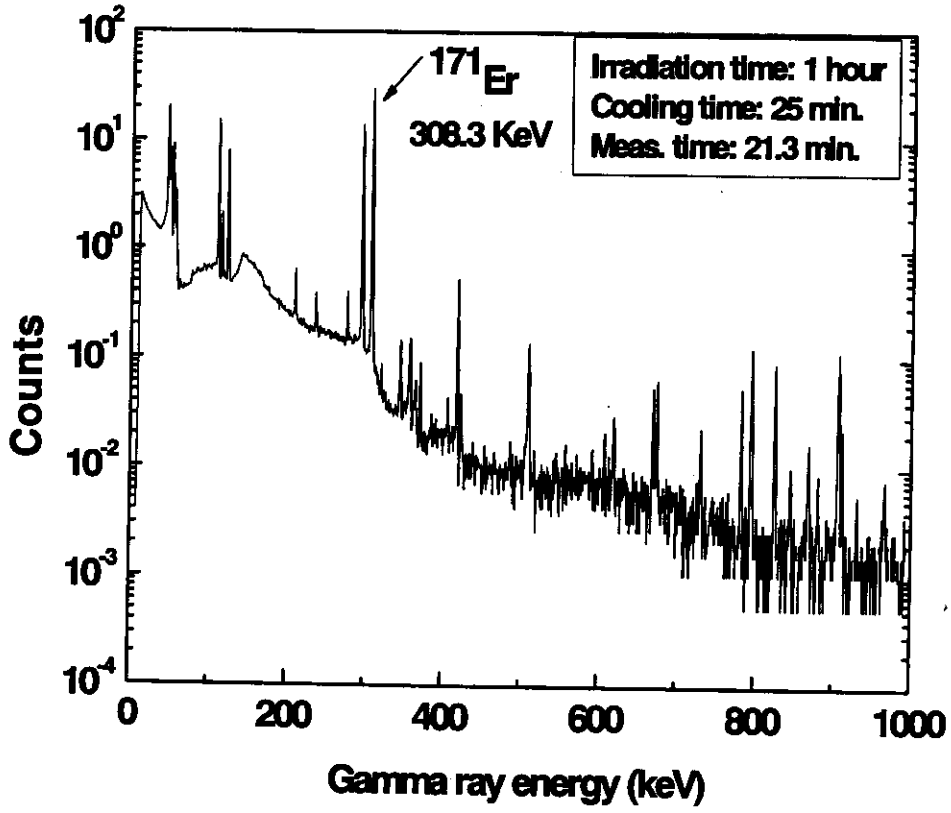

Fig. 4.7 An example of measured gamma rays spectrum of in the irradiated specimen of Er. Irradiation time: 1 hour, cooling time: 25 min. measurement time: 21.3 min.

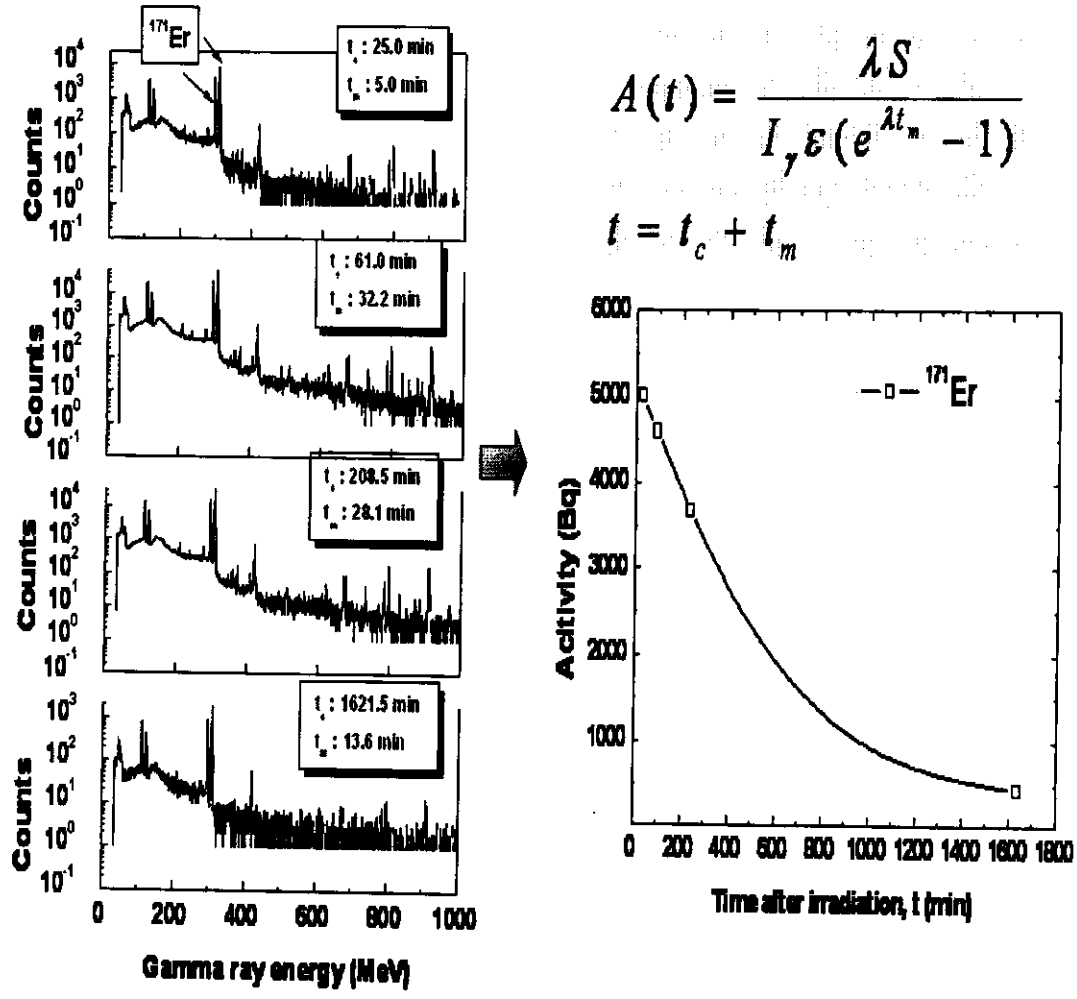

Fig. 4.8 Determination of activity of ^{171}Er as a function of time

The analysis procedure of the experiment was shown in Fig. 4.9. The neutron spectra at all locations were calculated with MCNP-4C code and JENDL-3.3 file. A special subroutine was used to represent the generation of neutrons in tritium-titanium target. Figure 4.10 shows the spectra at all locations. It can be seen that the neutron spectra at all locations have a dominant D-T peak, which is well-suited to investigating radiaonuclides generated through threshold type reaction with the high energy neutrons.

The spectra in Li mock-up case are similar to that of D-T case. The considerable low energy neutron flux including thermal neutrons flux are produced in case of Be mock-up. The spectra in Be/Li case are harder than those in Be mock-up case and softer than that in Li mock-up case.

Previous mock-up effort for induced radioactivity measurement using graphite and copper were conducted under ITER/EAD R&D Task T-218 [88,89]. Some neutron spectra controls simulating the fusion environments were carried out for the study of the shielding performance and tritium breeding performance of solid breeder [90-93]. This study is an unprecedented effort for evaluating neutron-induced radioactivity with large spectra change using liquid breeder relevant mock-ups.

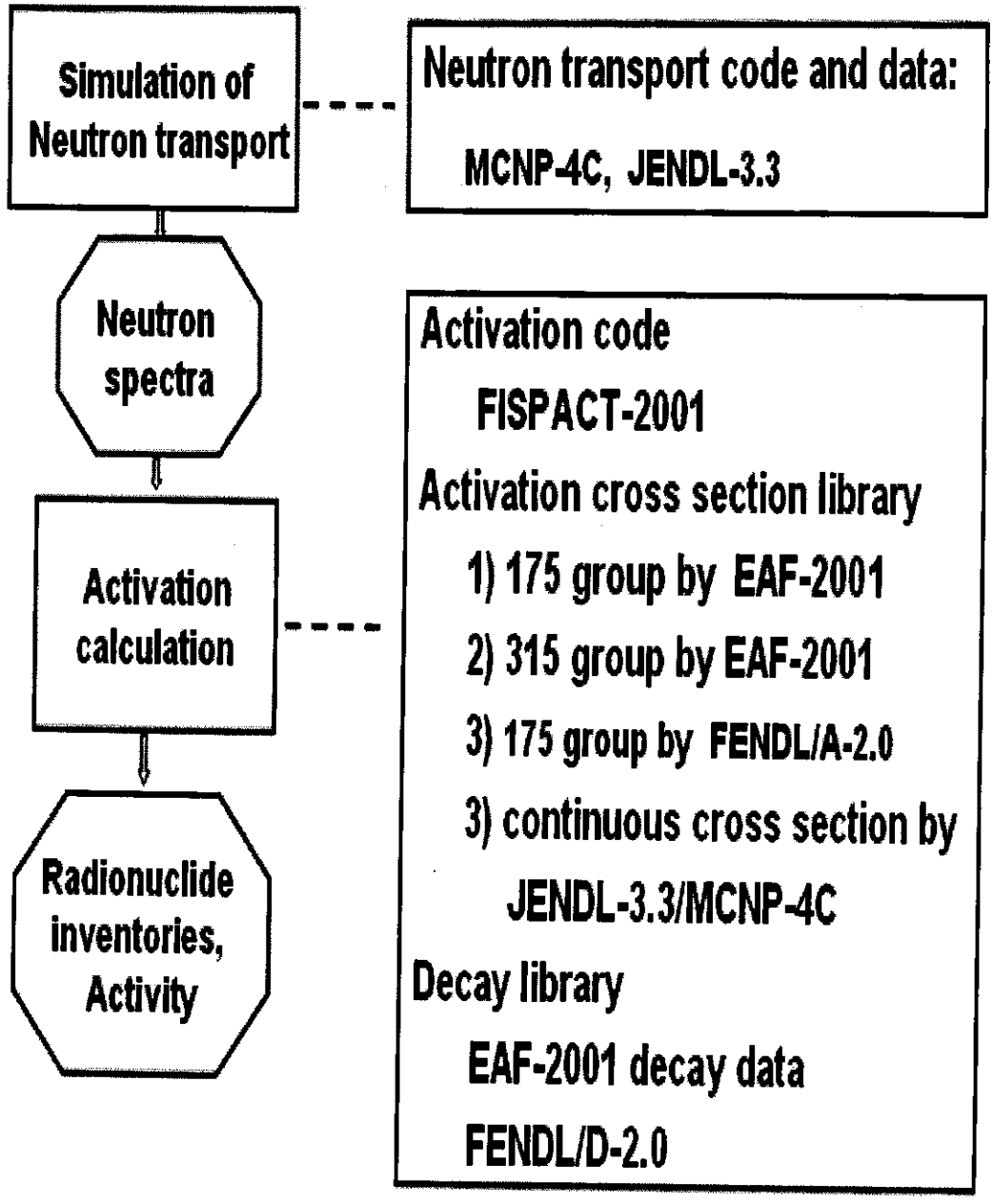

Fig 4.9 Procedure for analysis of the experiment

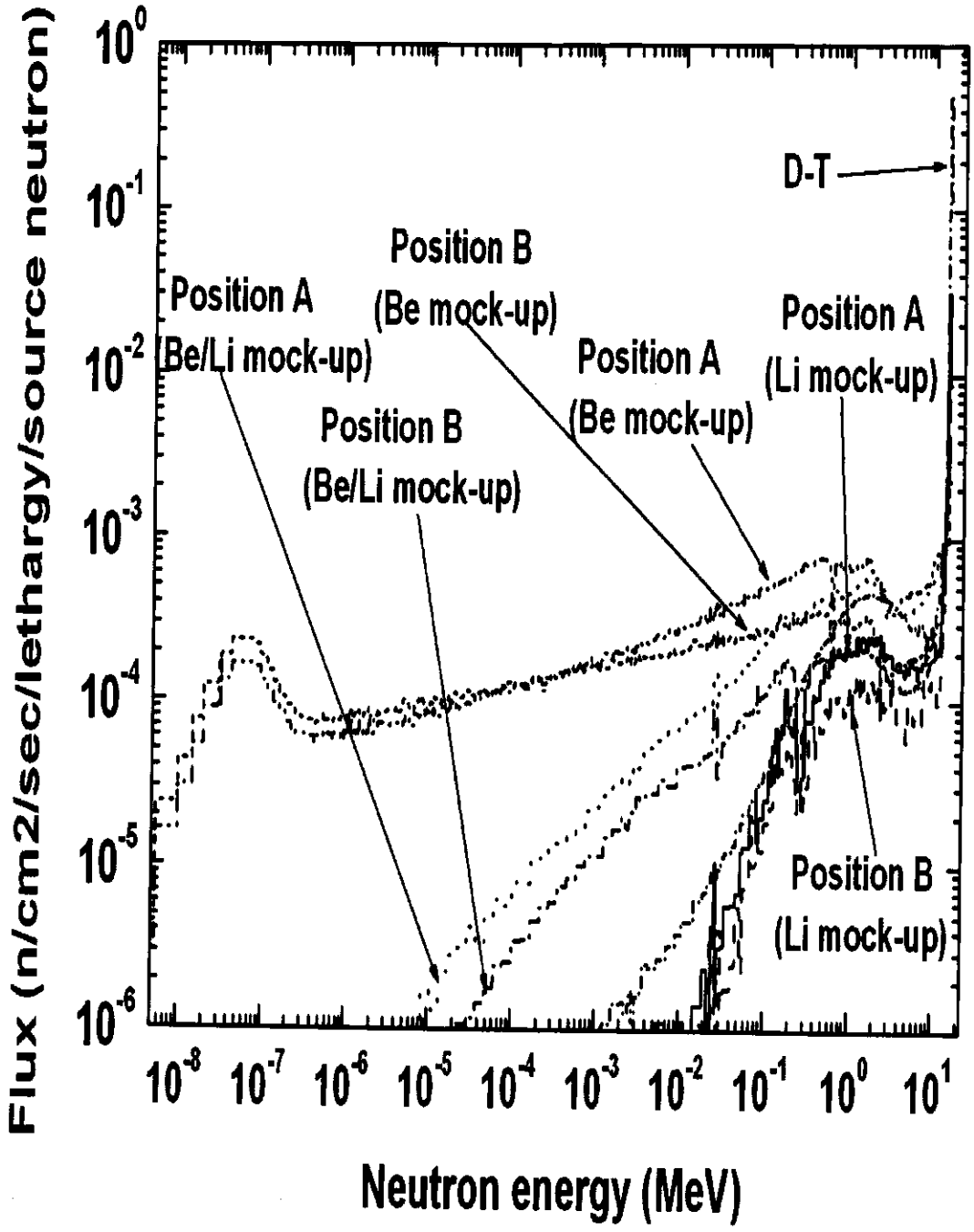

Fig. 4. 10 Neutron spectra at radiation locations in all cases

The absolute value of the total neutron flux at the specimens location was obtained by using the Nb foil via $^{93}Nb(n,2n)^{92m}Nb$ reaction whose cross section has been well-evaluated. The neutron flux at irradiation locations can be determined by the formula:

$$\phi = \frac{SM\lambda}{m\varepsilon\sigma I_\gamma N_A \exp(-\lambda t_c)(1-\exp(-\lambda t_m))(1-\exp(-\lambda t_i))} \quad (4.2)$$

Where

S is the peak counts,

M is atomic mass of niobium,

λ is the decay constant of ^{92m}Nb,

m is mass of niobium foil,

ε is detection efficiency,

σ is the effective cross section of $^{93}Nb(n,2n)^{92m}Nb$, with $\sigma = \frac{\int_0^\infty \sigma(E)\phi(E)dE}{\int_0^\infty \sigma(E)dE}$,

I_γ is probability of γ emitted,

N_A is Avgadro's number, 6.02×10^{23},

t_c is the cooling time,

t_m is elapsed measurement time,

t is irradiation time.

In the D-T and Li mock-up cases, most of the neutron flux is at high energy (>10 MeV) region. However, since there are significant low energy fractions of flux, the thin gold foils were used to measure and analyze the thermal neutron flux in Be and Be/Li mock-up cases. The reaction rate of $^{197}Au(n,$

γ)^{198}Au was obtained from the measured activity. The same reaction rate was calculated with MCNP-4C code and FENDL/E-2.0 file [94]. For Position A and B, the calculated reaction rates are in good agreement with the measured ones within 5% uncertainty for Be mock-up case.

Experimental analysis was performed with EASY-2001 including FISPACT-2001 code and EAF-2001 file. FENDL/A-2.0 activation cross section and FENDL/D-2.0 decay data libraries were also used in FISPACT calculation. The calculated neutron spectra in 175 and 315 energy structures were used as input files for activation calculation. Figure 4.11 shows the comparison of 175 group and 315 group structures. The 315 group structure has finer groups than 175 group structure in low energy range and nearly same group structure in high energy region.

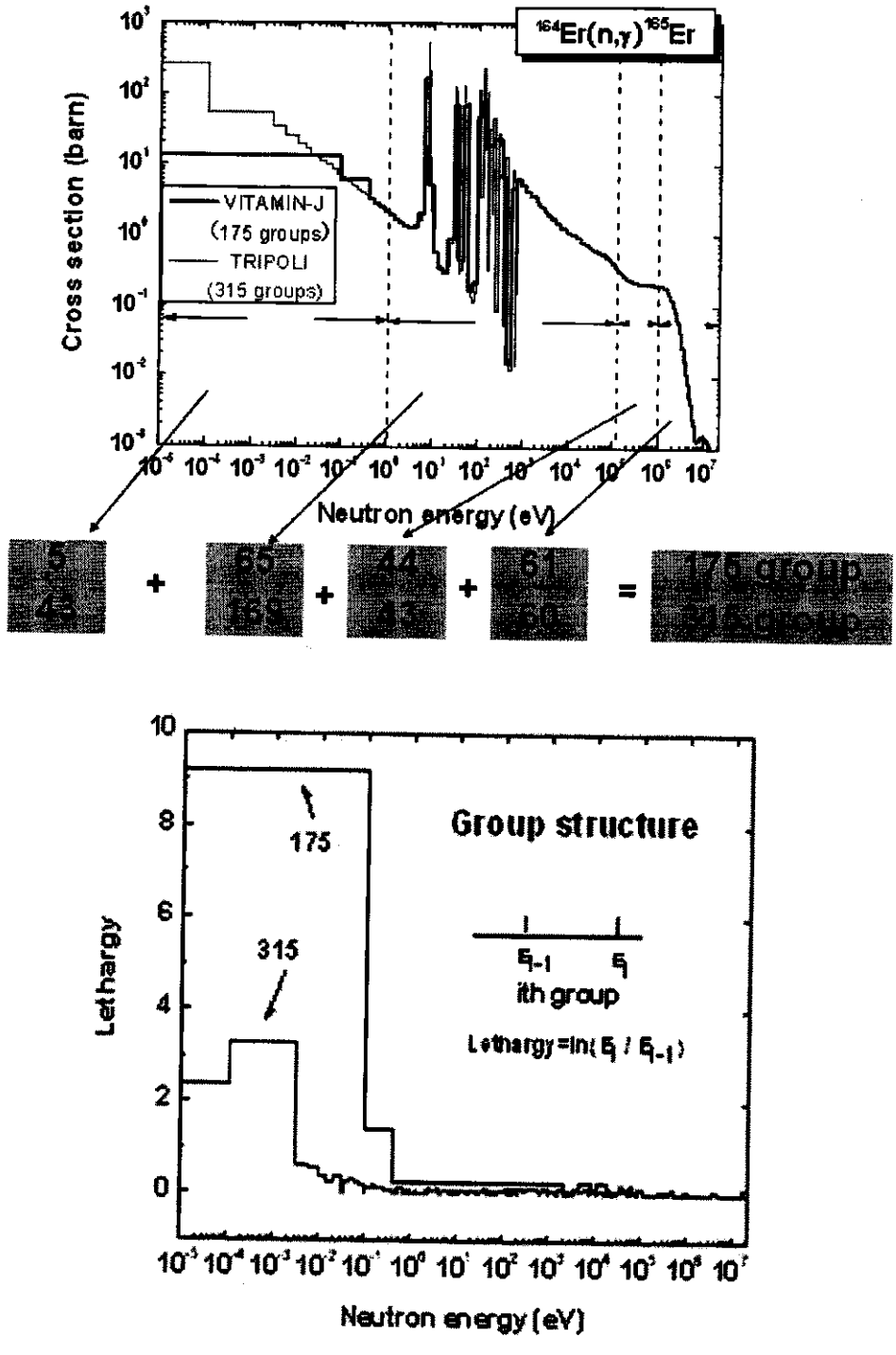

Fig. 4.11 175 group vs. 315 group structure

Table 4.3 lists the activation reaction of interest in the present study. There are two kinds of activation reactions: reactions without threshold energy e.g., ^{170}Er (n, γ); reactions with threshold e.g., ^{162}Er (n, 2n) ^{161}Er and ^{167}Er (n, p) ^{167}Ho.

Table 4.3 The reactions investigated in the present study

Specimen	Reaction	Type
Er	^{162}Er (n, 2n) ^{161}Er	Threshold (9.3 MeV)*
	^{167}Er (n, p) ^{167}Ho	Threshold (0.2 MeV)
	^{168}Er (n, d) ^{167}Ho	Threshold (5.8 MeV)
	^{168}Er (n, p) ^{168}Ho	Threshold (2.1 MeV)
	^{170}Er (n, γ) ^{171}Er	(n, γ)
Teflon	^{19}F (n, 2n) ^{18}F	Threshold (11.0 MeV)
NIFS-HEAT-2	^{51}V (n, p) ^{51}Ti	Threshold (1.7 MeV)
	^{51}V (n, γ) ^{52}V	(n, γ)
	^{51}V (n, α) ^{48}Sc	Threshold (2.1 MeV)
	^{48}Ti (n, p) ^{48}Sc	Threshold (3.3 MeV)

* Threshold energy

The measured activities of product nuclides were compared with the calculated values. Figure 4.12 shows the production of activity induced by neutron in irradiation phase and the comparison of activity between calculation and experiment. In irradiation phase, the activity increase with

irradiation time. If the neutron flux is constant, the neutron induced activity can be expressed as:

$$A_0=\Phi\,\sigma\,N\,(1-\exp(-\lambda\,t_i)) \qquad (4.4)$$

After irradiation, the activities were measured at different cooling times. The activation cross section σ can be examine by the comparison of activity between calculation and experiment.

During the irradiation, productions of D-T neutrons in tritium target fluctuate with time. Figure 4.13 shows an example of fluctuation of D-T neutrons recorded by MCS per 10 s. Since complex procedure is necessary for including the fluctuation effects in activation calculations, an irradiation with constant neutron flux needs to be assumed in the practical calculations. Therefore, the influence of the fluctuation was investigated in this study. The influence is a function of the irradiation history and half-lives of produced radioactive nuclides. The fluctuation R, which are the ratios of numbers of produced nuclides with the real irradiation conditions to those with constant flux. The values of R for various half-lives are calculated by formula:

$$R=\frac{\int_0^T \phi(t)\exp(-\lambda(T-t))dt}{\int_0^T \varphi_{const}\exp(-\lambda(T-t))dt} \qquad (4.5)$$

Where

T is the irradiation time,

ϕ (t) is the real neutron flux with fluctuation,

ϕ_{const} is the constant neutron flux, average of the flux in T:

$$\phi_{const} = \int_0^T \varphi(t)dt / T$$

λ is the decay constant of the produced nuclides.

The values of R for radionuclides are shown in Table 4.4 in all irradiation cases of the present study. It can be seen that the values of R are very close to unity except for ^{168}Ho. The calculated activity of ^{168}Ho should be decreased by ~3.5%.

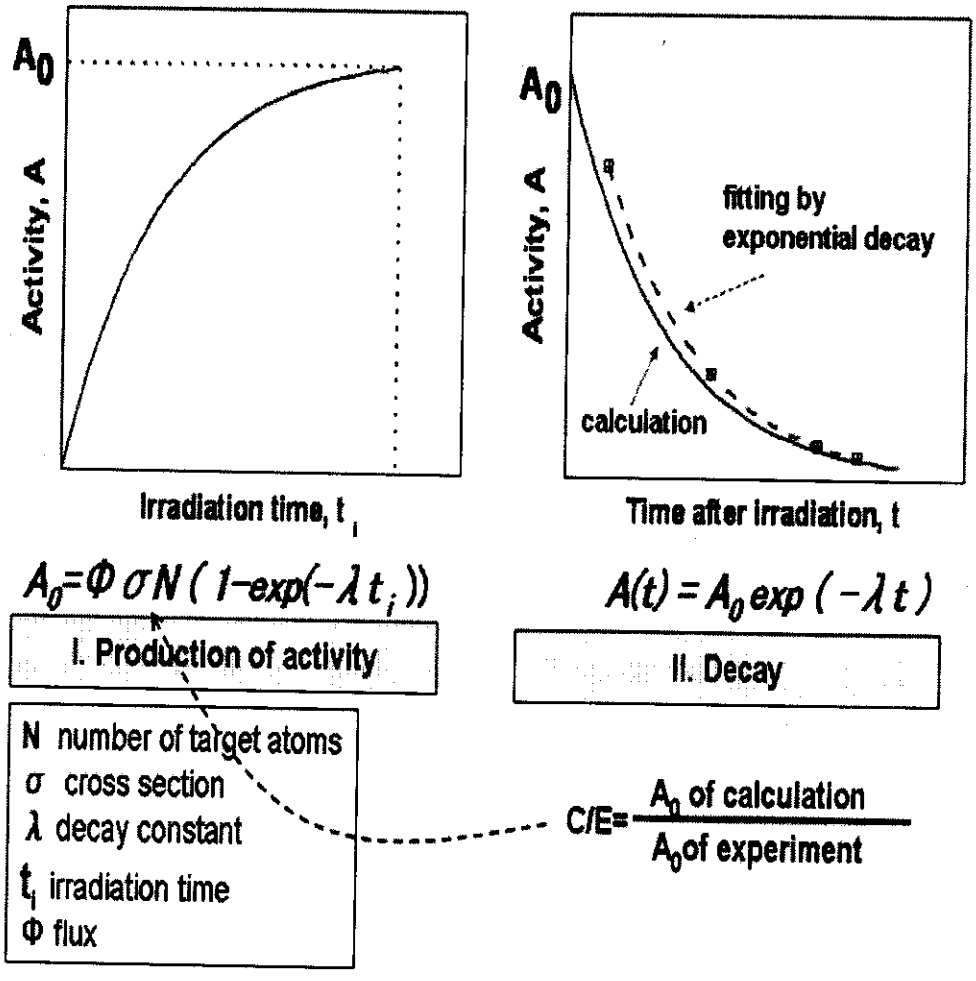

Fig.4.12 Neutron induced activity and the comparison of activity between calculation and experiment

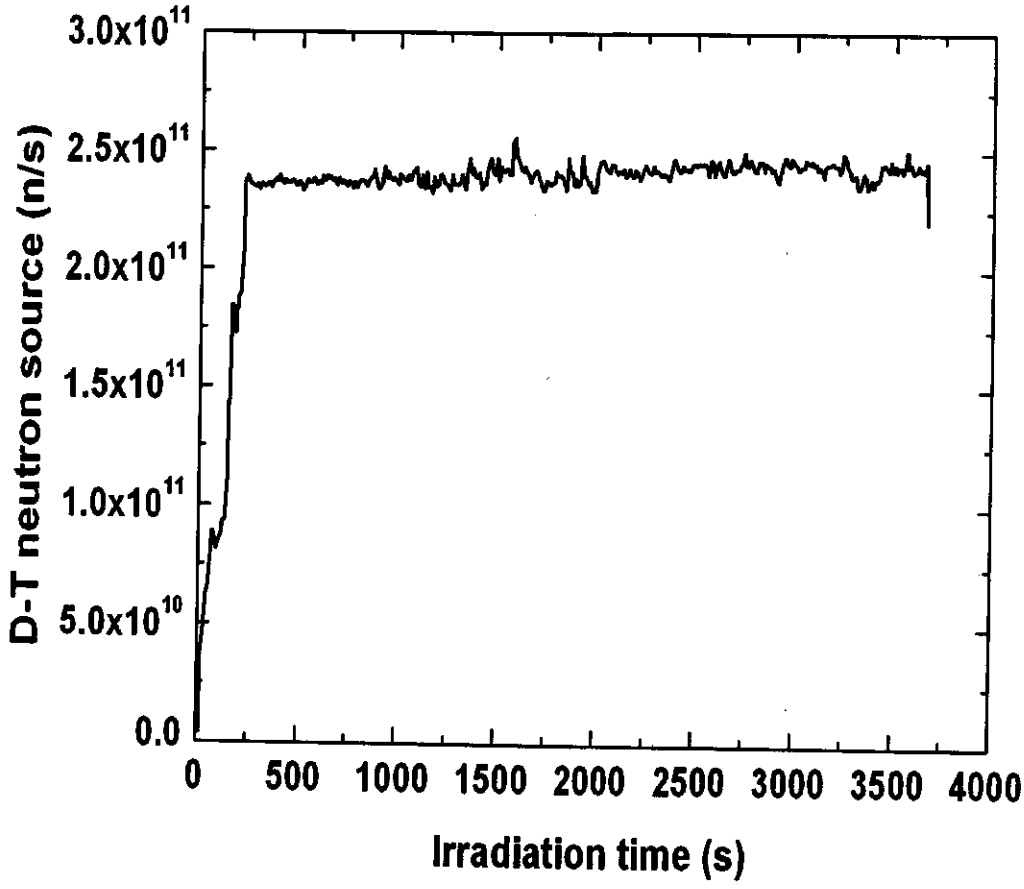

Fig. 4.13 An irradiation history of Er in Be mock-up case

Major sources for error are due to the gamma rays counting statistics, detector efficiency ($\sim$ 3%) and neutron flux determination. For most radionuclides, statistical errors of gamma rays counts are less than 1%. But for the case of ^{168}Ho, which causes relatively low count rate, statistical error extended to 4.6%. The major uncertainties in flux determination are from the

uncertainties of $^{93}Nb(n, 2n)^{92m}Nb$ cross section and neutron spectra. Overall experimental uncertainties are ~9% for D-T case and ~12% for mock-up cases.

Table 4.4 Estimates of R in the present experiments

	Values of R			
	D-T	Be mock-up	Li mock-up	Be/Li mock-up
^{167}Ho	0.999/20 m*	-	-	-
^{168}Ho	0.965/20 m	-	-	-
^{161}Er	0.999/20 m	1.004/1 h	0.998/1.7 h	0.999/2 h
^{51}Ti	0.999/6 m	0.999/20 m	1.000/20 m	1.003/20 m
^{48}Sc	0.999/2 h	-	0.984/ 2h	1.000/2 h
^{18}F	0.996/1 h	0.997/2 h	0.998/ 2.1 h	0.999/2 h
^{52}V	-	0.993/20 m	-	-
^{171}Er	-	1.002/1 h	-	-

* Values of R / irradiation time

4.3 Result and discussion

[I] High energy threshold reactions

The D-T peak is well suited to examine the activation with high energy threshold. The comparison between calculation and experiment (C/E) for the irradiation case I (D-T) are summarized in Table 4.5. The activities calculated with both EAF-2001 and FENDL/A-2.0 activation cross sections in 175 groups are compared with experiments. It can be seen that for the calculated activities with the two libraries agree well except for ^{167}Ho. There are three main activation paths for ^{167}Ho, namely ^{167}Er(n, p)^{167}Ho, ^{168}Er(n, d)^{167}Ho and ^{170}Er(n, α)^{167}Dy(β$^-$)^{167}Ho. Most of ^{167}Ho were originated from ^{167}Er(n, p)^{167}Ho. In the energy around 14 MeV, the three activation cross sections in EAF-2001 have higher values than those in FENDL/A-2.0. Especially for ^{168}Er(n, d)^{167}Ho, the difference of cross section values by almost one order was found in the energy around 14 MeV between the two libraries. The detailed check for the three activation cross sections is remaining to be performed.

An overall plot of C/E values for the products of radionuclides through high energy threshold reaction for all locations was shown in Fig. 4.14. The C/E values were calculated with EAF-2001 activation cross sections in 175 groups. Data for ^{167}Ho and ^{168}Ho in the mock-up cases cannot be derived because of insufficient high energy neutron fluence. For most nuclides the C/E values lie in the band of 0.8-1.2. However, a significant underestimation for ^{168}Ho was found in D-T neutron irradiation case. Figure 4.14 shows the

D-T peak and $^{168}Er(n, p)^{168}Ho$ cross section. The effective threshold energy is near 14 MeV and the cross section rise steeply around 14 MeV. The analysis with 315 group cross section and continuous section data derived by dividing the $^{168}Er(n, p)^{168}Ho$ reaction rates calculated by MCNP-4C code with JENDL3.3 were also performed for ^{168}Ho. The values of C/E of ^{168}Ho calculated with 175, 315 group and continuous data were 0.62, 0.62 and 1.15, respectively. There is no improvement with 315 group data for ^{168}Ho, production of threshold reaction because of the nearly same group structure as 175 group at >0.1 MeV as shown in Fig. 4.11. C/E of ^{168}Ho calculated with continuous data was increased to 1.15.

Table 4.5 C/E values of activities induced in specimens in D-T irradiation case for threshold activation reaction

Specimen	Product	Calculation/experiment (C/E)	
		EAF-2001 (175 groups)	FENDL/A-2.0 &FENDL/D-2.0 (175 groups)
Er	^{167}Ho	1.22	1.10
	^{168}Ho	0.62	0.60
	^{161}Er	0.97	0.97
NIFS-HEAT2 (V-4Cr-4Ti)	^{51}Ti	1.14	1.15
	^{48}Sc	1.03	1.08
Teflon(CF_2)	^{18}F	1.02	0.99

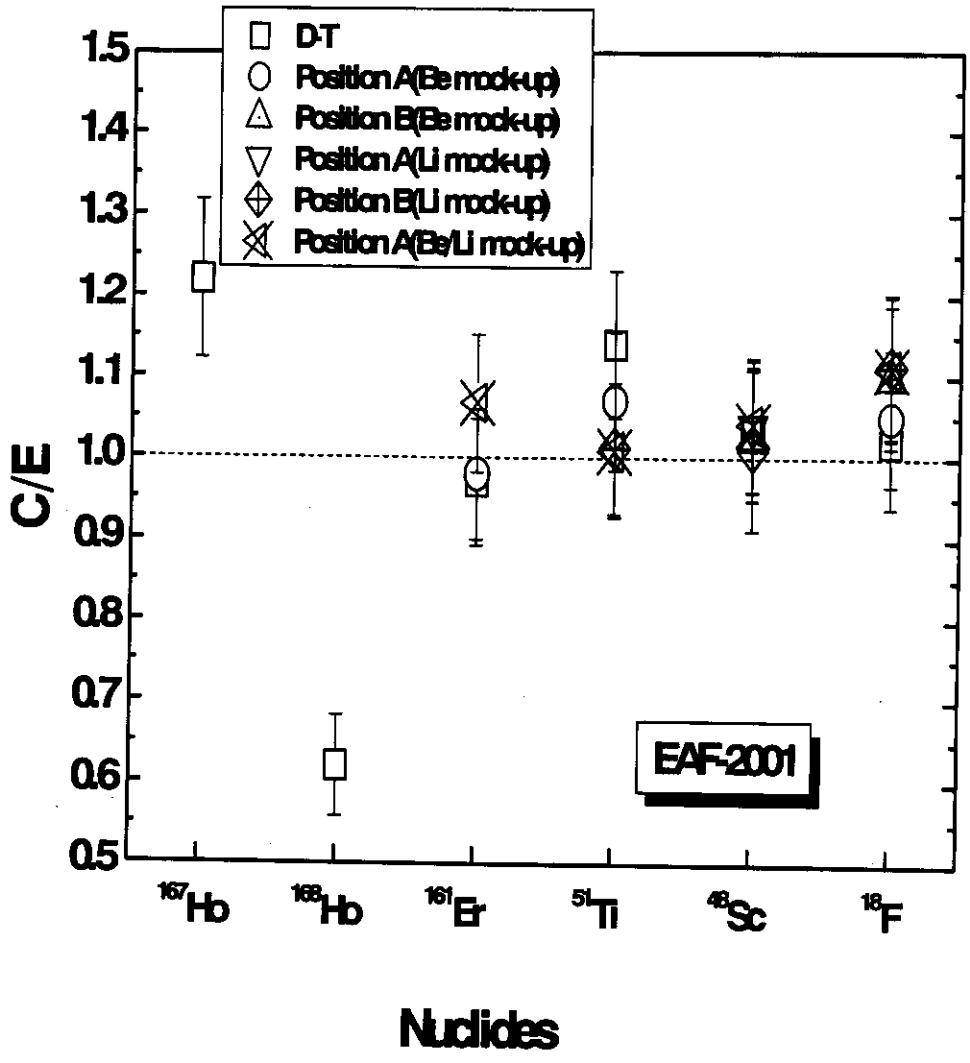

Fig.4.14 C/E for various radionuclides produced by high energy threshold activation reactions

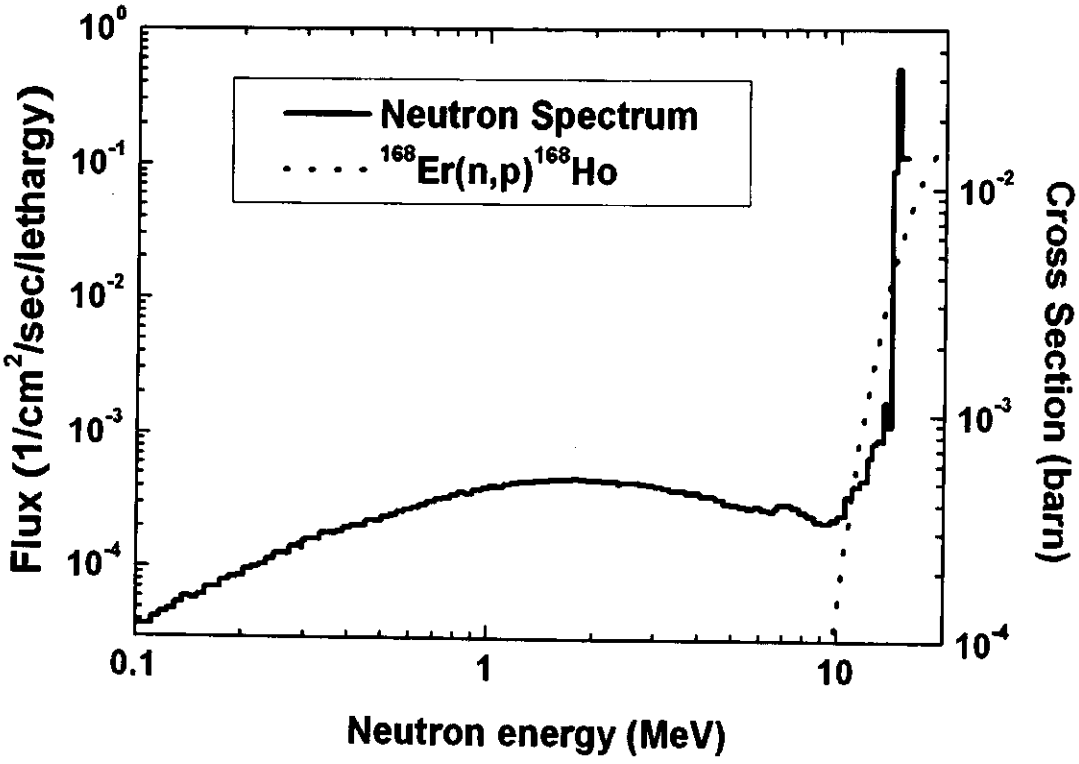

Fig.4.15 D-T neutron peak and ^{168}Er(n, p)^{168}Ho cross section

[II] (n, γ) reactions

Table 4.6 lists the C/E values of ^{171}Er and ^{52}V calculated with 175 group cross section. The overestimation for ^{52}V and ^{171}Er, product of (n, γ), were found using the activation cross section in 175 groups. In Be mock-up case the 315 group activation cross sections of EAF-2001 were also used for the analysis for ^{52}V and ^{171}Er. For the purpose of examining the grouping effect, the activation calculation with continuous cross sections were conducted by replacing the activation cross section of ^{51}V(n, γ)^{52}V and ^{170}Er(n, γ)^{171}Er in groups with the effective cross sections. The effective cross section of ^{51}V(n, γ)^{52}V and ^{170}Er(n, γ)^{171}Er were derived by dividing the (n, γ) reaction rates

calculated by MCNP-4C code with JENDL3.3.

Table 4.6 C/E values of the induced activities of ^{171}Er, ^{52}V, in the case of Be and Be/Li mock-ups

Specimen	Product	C/E		
Specimen	Product	Position A (Be mock-up)	Position A (Be mock-up)	Position A (Be/Li mock-up)
Er	^{171}Er	1.28	1.23	1.35
NIFS-HEAT-2	^{52}V	1.10	1.06	-

The comparisons of energy group effects were shown in Fig. 4.16. For ^{52}V, the contribution from $^{51}V(n, \gamma)$ reaction with neutrons in the range below 0.53 eV and 0.53eV-111 keV are ~80% and ~20%, respectively. Using 315 group cross sections, C/E values of ^{52}V show a clear trend approaching to unity because of the finer group structures in the range <0.53 eV. The results also agree well with the case using the continuous cross section.

In Be mock-up case more than 70% of ^{171}Er were originated from $^{170}Er(n, \gamma)$ reaction with neutrons in 0.53 eV-111 keV. The improvement in overall C/E of ^{171}Er with 315 group activation cross sections is insignificant. For the reaction, there is a huge resonance peak at 95 keV as shown in Fig 4.17. The large overestimation for the calculation with 315 groups compared to that with continuous cross section is thus due to the coarse grouping around the resonance peak. For the case of Be/Li mock-up, most of ^{171}Er were generated at resonance range because of very low flux of neutrons with <~10^{-6} MeV

where the average cross section is relatively large. In this case, large discrepancy was observed even with continuous cross section. The reason would be the uncertainty in estimation of spectra and the cross section in this resonance range according to the rapid increase in neutron flux with the energy in the resonance range as seen in Fig. 4.17.

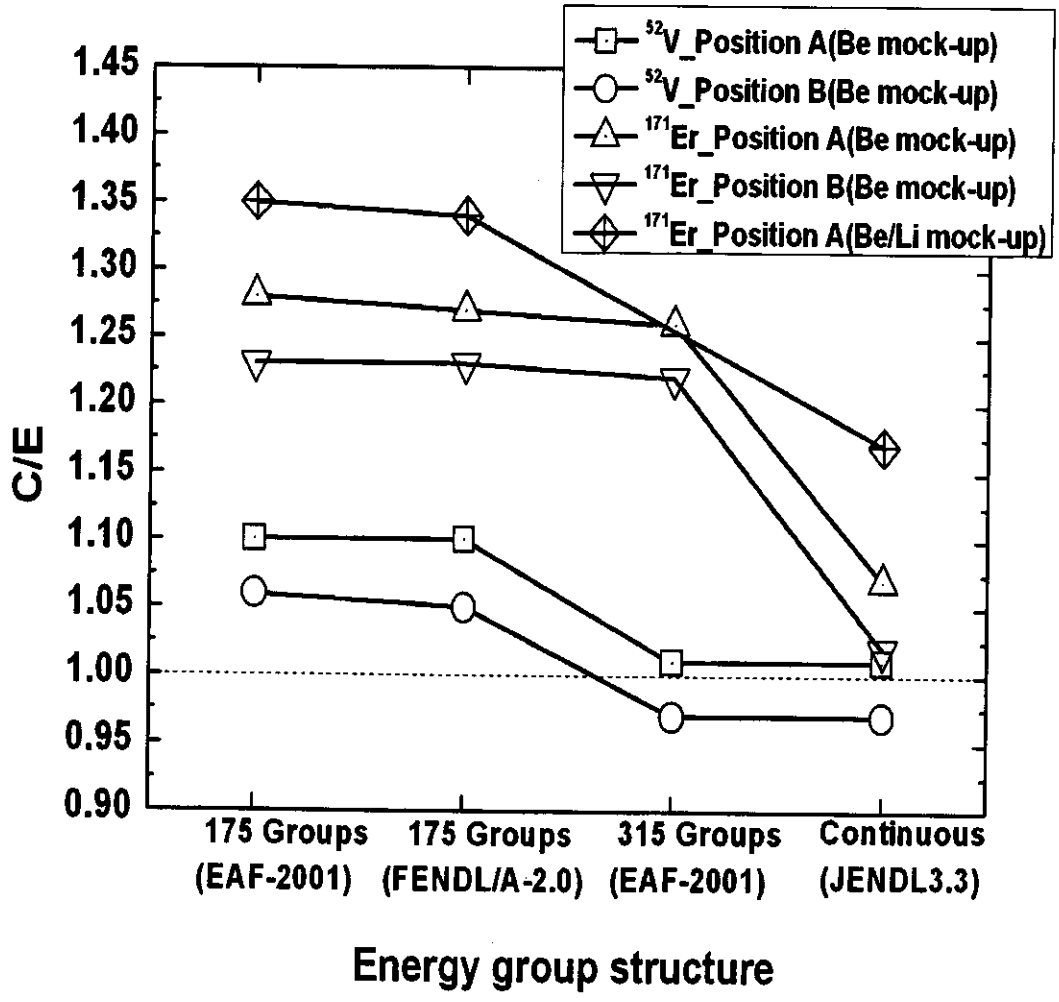

Fig. 4.16 Energy group effect on the activation calculations for ^{52}V and ^{171}Er

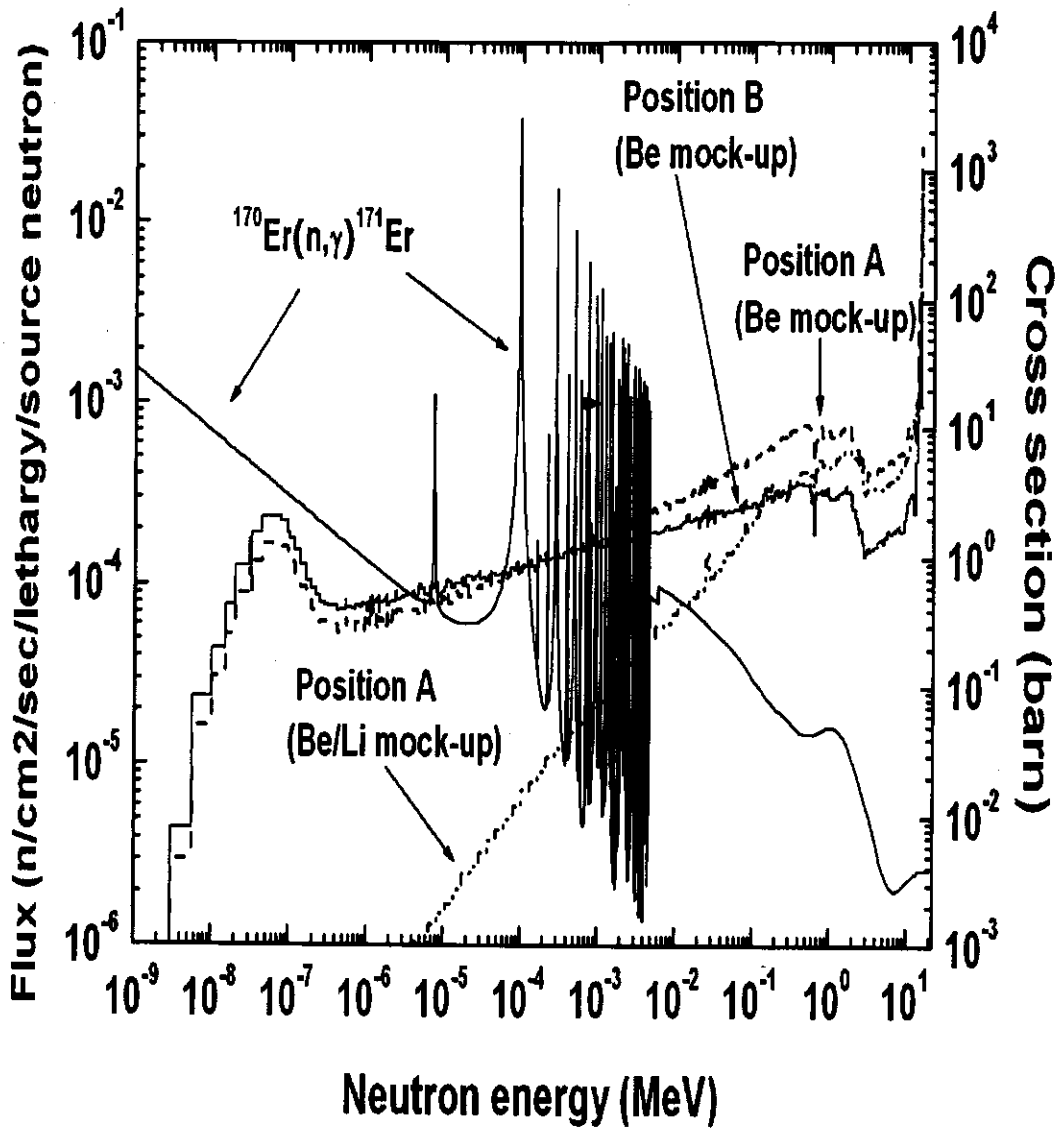

Fig. 4.17 The $^{170}Er(n, \gamma)^{171}Er$ cross section and the neutron flux spectra in the Be mock-up and Be/Li mock-up cases.

4.4 Summary

A series of irradiation assemblies were built to generate the neutron fields simulating the prototypical fusion neutron spectra in various blankets. The irradiations were conducted to investigate the activation of materials relevant to Lithium/vanadium-alloy and Flibe/vanadium-alloy blankets. The measured activities of various radionuclides were compared with the calculations. The effects of grouping of the cross section depend on the type of reaction, threshold energy and resonance peaks, if any, and neutron spectra.

The Summary of the recommendation derived in this study is shown in Table 4.7. The reactions were categorized into the threshold and the (n, γ) reactions, the former then divided into two groups according to the cross section change around 14 MeV, and the later according to the resonance.

However the activities of some important activation productions in FFHR e.g. ^{166m}Ho, have not been measured in the present study due to low activities. Further investigation for the activation cross sections for the important radionuclides in FFHR (indicated in Table 4.7 in underline) is still required.

Table 4.7 Summary of the necessary cross-section data

Type of reactions	Example for FNS experiment analyzes	Example for FFHR activation analyzes	Necessary cross section data		
			D-T, Li mock-up	Be/Li mock-up	Be mock-up
			Li blanket	Li/Be blanket	Flibe blanket
Threshold reaction without large change of cross section around 14 MeV	$^{51}V(n, p)^{51}Ti$ $^{51}V(n, \alpha)^{48}Sc$ $^{48}Ti(n, p)^{48}Sc$ $^{19}F(n, 2n)^{18}F$ $^{162}Er(n,2n)^{161}Er$ $^{167}Er(n, p)^{167}Ho$ $^{168}Er(n, d)^{167}Ho$	$^{51}V(n, p)^{51}Ti$ $^{51}V(n, \alpha)^{48}Sc$ $^{48}Ti(n, p)^{48}Sc$ $^{19}F(n, 2n)^{18}F$ $^{46}Ti(n, p)^{46}Sc$ $^{47}Ti(n, p)^{47}Sc$ $^{50}Cr(n, d)^{49}V$ $^{170}Er(n,2n)^{169}Er$ $^{169}Tm(n,p)^{168}Tm$ $^{166}Er(n,2n)^{165}Er$	175 group	175 group	175 group
Threshold reaction with large change of cross section around 14 MeV	$^{168}Er(n, p)^{168}Ho$	$^{166}Er(n,p)^{166m}Ho$	continuous*	continuous*	continuous*
(n, γ) without large resonance	$^{51}V(n, \gamma)^{52}V$	$^{51}V(n, \gamma)^{52}V$ $^{171}Tm(n,\gamma)^{172}Tm$	175 group	315 group	315 group
(n, γ) with large resonance	$^{170}Er(n, \gamma)^{171}E$	$^{170}Er(n, \gamma)^{171}Er$ $^{165}Ho(n,\gamma)^{166m}Ho$ $^{168}Er(n, \gamma)^{169}Er$ $^{164}Er(n, \gamma)^{165}Er$ $^{169}Tm(n,\gamma)^{170}Tm$	175 group	continuous**	continuous

* Accurate estimate of neutron spectra and cross section may be necessary in the case of very large change of the cross section around 14 MeV

** Accurate estimate of neutron spectra is also necessary

Underline: necessary for FFHR analysis but not examined in this study

CHAPTER 5

Conclusions

The objectives of the present study are to investigate Li and Flibe blankets for FFHR2m by neutronics analysis and to examine or improve the neutronics calculation procedure for application to liquid blankets by comparison with activation experiment with D-T neutrons.

The neutronics analysis for liquid blankets, Li/V, Li/Be/V, Flibe/V and Flibe/Be/V, were performed for FFHR2 design. The impact of the external Be on the tritium breeding, shielding and the associated activation issues of Li and Flibe blankets for FFHR2m design were investigated.

For the purpose of verifying or improving the neutronics calculation procedure, especially for activation application to liquid blankets, a series of irradiation experiments were performed using Fusion Neutronics Source (FNS) at JAEA and activation of materials relevant to Lithium/vanadium-alloy and Flibe/vanadium-alloy blankets were investigated.

Conclusions of the present study are:

A) Detailed neutronics characterization of Li and Flibe blankets using V-alloy structure for FFHR has, for the first time, been carried out:

A-1) Advantage of the use of Be is quantified. With Be, TBR design margin for Li and Flibe blankes could be improved. For Li blanket with Be, the shielding design margin could also be improved with adequate TBR. The results provide information necessary for characterizing trade-off of using Be in Li and Flibe blankets.

A-2) The Er_2O_3 coating induces the long-term radioactivity of Li blanket. However, recycle of structural materials is still feasible with Er_2O_3 coating in 10 μm thickness. Thinner Er_2O_3 coating is necessary for realizing

hands-on recycling.

B) Experimental studies of activation characteristics for materials in Li and Flibe blankets have been carried out using a D-T neutron source, especially for the first time for the Er_2O_3 coating:

B-1) For the threshold reactions, where the threshold energy is close 14 MeV and its cross-section rises steeply around 14 MeV, continuous-energy cross-section data is needed.

B-2) For the (n, γ) reaction with high cross-section at thermal neutrons region, finer grouping is necessary.

B-3) Use of continuous-energy cross-section is necessary for (n, γ) reaction with dominant resonance peak in medium energy ranges.

B-4) The cross section data of $^{170}Er(n, \gamma)^{171}Er$ needs re-evaluation.

REFERENCE

[1] Jose Goldemberg et al., "Renewable energy-traditional biomass vs. modern biomass", Energy Policy 32 (2004) 711–714

[2] Donald L. Klass, "A critical assessment of renewable energy usage in the USA", Energy Policy 31 (2003) 353–367

[3] R. Toschi, "Nuclear fusion, an energy source", Fusion Eng. Des., 36 (1997) 1-8

[4] The promise of fusion energy, http://fusioned.gat.com/images/pdf/promise_of_fusion.pdf

[5] Chris Llewellyn Smith, "The need for fusion", Fusion Eng. Des., 74 (2005) 3-8

[6] J.A. Schmidt, J.M. Ogden, "Fusion power deployment", Fusion Eng. Des., 63-64 (2002) 19-23

[7] Yolanda Lechon, et al., "A global energy with fusion", Fusion Eng. Des., 75-79 (2005) 1141-1144

[8] Koji Tokimatsu, et al., "Role of nuclear fusion in future energy systems and environment under future uncertainties", Energy policy 31 (2003) 775-797

[9] Karine Fiore, "Nuclear energy sustainability: Understanding ITER", Energy policy 34 (2006) 3334-3341

[10] Ronald L. Miller, "Economic goals and requirements for competitive fusion energy", Fusion Eng. Des., 41 (1998) 393-400

[11] J. Ongena, G. Van Oost, "Energy for Future Centuries: Will Fusion Be an Inexhaustible, Safe, and Clean Energy Source?", Fusion Science and Technology 45 Number 2T • (2004) 3-14

[12] J. Ongena, G. Van Oost, "Energy for Future Centuries - Prospects for Fusion Power as a Future Energy Source", Fusion Science and Technology 49 (2006) 3-15

[13] B J Bickerton, "The purpose, status and future of fusion research", Plasma Phys. Control. Fusion 35 (1993) B3-B21

[14] John Lilley, "Nuclear Physics-Physics-Principles and Applications", Copyright@ 2001 by John Willey & Sons Ltd. p. 299

[15] R.M. White et al., "FENDL/C-2.0. Chargedparticle reaction data library for fusion applications", summary documentation by A.B. Pashchenko

and H. Wienke, report IAEA-NDS- 77, IAEA, March 1997. Data library retrieved online (or: received on tape) from the IAEA Nuclear Data Section.

[16] ITER homepage http:// www.iter.org.

[17] P.-H. Rebut, "ITER: the first experimental fusion reactor", Fusion Eng. Des. 27 (1995) 3-16

[18] R. Aymar, "ITER overview", Fusion Eng. Des. 36 (1997) 9-21

[19] Hiroshi Mattsumoto and Pietro Barabaschi, "Prediction of performance in ITER-FEAT", Fusion Science and Technology 40 (2001) 37-51

[20] R. Aymar, "Status of ITER ", Fusion Eng. Des. 61-62 (2002) 5-12

[21] Y. Shimomura, "Preparation of ITER construction and operation", Fusion Eng. Des. 81 (2006) 3-31

[22] M. Mori et al., "Japanese activities in ITER transitional arrangements", Fusion Eng. Des. 81 (2006) 69-77

[23] V.A. Belyakov et al., "Russia Federation contribution to the ITER project", Fusion Eng. Des. 81 (2006) 79-86

[24] Ned R. Sauthoff, "U.S. contribution to ITER", Fusion Eng. Des. 81 (2006) 87-92

[25] R. Aymar, "The ITER reduced cost design", Fusion Eng. Des. 49-50 (2000) 13-25

[26] L. Giancarli et al., "Breeding Blanket Modules testing in ITER: An international program on the way to DEMO", Fusion Eng. Des. 81 (2006) 393-405

[27] M..Z. Youssel and M.E. Sawan, "On the strategy and requirements for neutronics testing in ITER", Fusion Science and Technology 47 (2005) 1038-1045

[28] I.R. Kirillov et al., "RF TBMs for ITER tests", Fusion Eng. Des. 81 (2006) 425-432

[29] H. Neuberger et al., "Integration of the EU HCPB Test Blanket Modules system in ITER", Fusion Eng. Des. 81 (2006) 499-503

[30] K.M. Feng et al., "Preliminary design for a China ITER test blanket module" Fusion Eng. Des. 81 (2006)1219-1224

[31] Kikio Enoeda et al., "Overview of design and R&D of test blanket in Japan", Fusion Eng. Des. 81 (2006) 415-424

[32] Karl Ehrlich, "Materials research towards a fusion reactor", Fusion Eng. Des. 56-57 (2001) 71-82

[33] T. Muroga et al., "Overview of materials research for fusion reactors", Fusion Eng. Des. 61-62 (2002) 13-25

[34] Dale L. Smith et al., "Overview of the blanket comparison and selection study", Fusion Technology 8 (1985) 10-44

[35] T. Muroga et al., "Vanadium alloys-overview and recent results", Journal of Nuclear Materials 307-311 (2002) 547-554

[36] Nagasaha Takuya et al., "Low activation characteristics of several heats of V-4Cr-4Ti ingot", J. Plasma Fusion Res. SERIES 5 (2002) 545-550

[37] T. Muroga et al., "Characterization for fusion candidate vanadium alloys", Plasma Science & Technology 6 (2004) 2395-2399

[38] S. Sharaft et al., "Status and prospects for SiC-SiC composite materials development for fusion applications", Fusion Eng. Des. 29 (1995) 411-420

[39] L. Giancarli et al., "R&D issues for SiC_f/SiC composites structural material in fusion power reactor blankets", Fusion Eng. Des. 48 (2000) 509-520

[40] J.B.J. Hegeman et al., "Mechanical and thermal properties of SiC_f/SiC composites irradiated with neutrons at high temperatures" Fusion Eng. Des. 75-79 (2005) 789-793

[41] E. Proust et al., "Solid breeder blanket design and tritium breeding", Fusion Eng. Des. 16 (1991) 73-84

[42] N. Roux et al., "Ceramic breeder material development", Fusion Eng. Des. 41 (1998) 31-38

[43] Claudio Nardi et al., " A breeding blanket in ITER-FEAT", Fusion Eng. Des. 69 (2003) 315-319

[44] J.W. Davis et al., "Thermal diffusivity/conductivity of AECL Li_2TiO_3 ceramic", J. Nucl. Mater. 232 (1996) 65-68

[45] S. Malang et al., "Crucial issues on liquid blanket design", Fusion Eng. Des. 16 (1991) 95-109

[46] S. Malang et al., "Comparison of lithium and eutectic lead-lithium alloy, two candiadate liquid metal breeder materials for self-cooled blankets", Fusion Eng. Des. 27 (1995) 399-406

[47] B.A. Pint "Liquid metal compatibility issues for test blanket modules", Fusion Eng. Des. 81 (2006) 901-908

[48] David A. Petti et al.,, "JUPITER-II motlten salt Flibe reseach: An

update on tritium, mobilization and redox chemistry experiments", Fusion Technology, 81 (2006) 1439-1449.

[49] H. Moriyama et al., "Molten salts in fusion nuclear technology", Fusion Technology, 39-40 (1998) 627-637.

[50] C.P.C Wong et al., "Helium cooling of fusion reactors", Fusion Eng. Des. 25 (1994) 249-262

[51] A. Ying et al., "An overview of US ITER test blanket module program", Fusion Eng. Des. 81 (2006) 433-441

[52] L.V. Boccaccini et al., "Test strategy for the European HCPB test blanket module in ITER", Fusion Science and Technology 47 (2005) 1015-1022

[53] Mikio Enoeda et al., "Development of solid breeder blanket at JAERI", Fusion Science and Technology 47 (2005) 1060-1067

[54] I.R. Kirillov et al., "Liquid lithium self-cooled breeding blanket design for ITER", Fusion Eng. Des. 39-40 (1998) 669-674

[55] Dong Won Lee et al., "Preliminary design of a helium cooled molten lithium test blanket module for the ITER test in Korea", Fusion Eng. Des. 82 (2007) 381-388

[56] C.P.C. Wong et al., "Assessment of first wall and blanket options with the use of liquid breeder", Fusion Science and Technology 47 (2005) 502-508

[57] Yasushi Seki, "Overview of the Japanese fusion reactor studies program", Fusion Eng. Des. 48 (2000) 247-254

[58] A. Sagara et al., "Blanket and divertor design for force free helical reactor (FFHR)", Fusion Eng. Des. 29 (1995) 51-56

[59] A. Sagara et al., "Blanket design using Flibe in helical-type fusion reactor FFHR", Journal of Nuclear materials 248 (1997) 147-152

[60] http://www.nifs.ac.jp/NIFS-NEWS/pdf/167-1.pdf

[61] A. Sagara et al., "Design and development of the Flibe blanket for helical-type fusion reactor FFHR", Fusion Eng. Des. 49-50 (2000) 661-666

[62] A. Sagara et al., "Improved structure and long-life blanket concepts for heliotron reactors", Nuclear Fusion 45 (2005) 258-263

[63] R.F. Mattas et al., "Results of R&D for lithium/vanadium breeding blanket design", Fusion Eng. Des. 39-40 (1998) 659-668

[64] D. -K. Sze, "IPFR, integrated pool fusion reactor concept", Fusion

Technology, 10 (1986) 875-880.
[65] Z. Yao et al.,, "In situ formation and chemical stability of Er_2O_3 coating on V-4Cr-4Ti in liquid lithium", Fusion Eng. Des. 75-79 (2005) 1015-1019.
[66] Z. Yao et al.,, "The in situ growth of Er_2O_3 coating on V-4Cr-4Ti in liquid lithium", Fusion Eng. Des. 81 (2006) 951-956
[67] Muroga, T. et al., "Blanket neutronics of Li/vanadium-alloy and Flibe/vanadium-alloy systems for FFHR", Fusion Eng. Des. 81 (2006) 1203-1209
[68] T. Tanaka et al., "Tritium self-sufficiency and neutron shielding performance of self-cooled liquid blanket system for helical reactor", Fusion Sci. Techno. 47 (2005) 530-534.
[69] L.N. Topilski et al., "Validation and benchmarking in support of ITER-FEAT safety analysis", Fusion Eng. Des. 54 (2001) 627-633
[70] J. F. Briesmeister, MCNP-A general Monte Carlo n-particle transport code, LA-12625-M, 2000
[71] R.A. Forrest, "The European activation system: EASY-2001 overview", UKAEA Report, UKAEA FUS 449 (2001)
[72] R.A. Forrest, "FISPACT-2001: User Manual", UKAEA Report, UKAEA FUS 450 (2001)
[73] R.A. Forrest et al., "The European activation file: EAF-2001 cross section library", UKAEA Report, UKAEA FUS 451 (2001)
[74] R.A. Forrest et al., "The European activation file: EAF-2001 decay data library", UKAEA Report, UKAEA FUS 452 (2001)
[75] T. Tanaka et al., "Development of three-dimensional neutronics calculation system for design studies on helical reactor FFHR", Fusion Eng. Des. 81 (2006) 2761-2766
[76] M.A. Abdou et al., "Deuterium-tritium fuel self-sufficiency in fusion reactors", Fusion Technology 9 (1986) 250-285
[77] M.Z. Youssef et al., "Uncertainties in the prediction of tritium breeding in candidate blanket designs due to present uncertainties in nuclear data base", Fusion Technology 9 (1986) 286-307
[78] L.A. El-Guebaly, "Neutronics assessment for the ARIES advanced reactor studies", Fusion Eng. Des. 28 (1995) 658-664
[79] L.A. El-Guebaly et al., "Nuclear issues and analysis for ARIES spherical and advanced tokamaks", Fusion Eng. Des. 51-52 (2000)

325-330
[80] T. Noda et al., "Induced activity and damage of superconducting aterials for a fusion reactor", Fusion Eng. Des. 81 (2006) 1033-1037
[81] K. Humer et al., "Radiation effects on the mechanical properties of insulators for fusion magnets", Fusion Eng. Des. 81 (2006) 2433-2441
[82] Mohamed E. Sawan, Peter L. Walstrom, "Superconducting Magnet Radiation Effect in Fusion Reactors", Fusion Technology, 10 (1986) 741-746
[83] T. NAKAGAWA et al., "Japanese Evaluated Nuclear Data Library Version 3 Revision-2:JENDEL-3.2", J. Nucl. Sci. Technol., 32(12) (1995) 1259
[84] K. Shibata et al., "Japanese Evaluated Nuclear Data Library Version 3 Revision-3: JENDL-3.3," J. Nucl. Sci. Techno., 39, (2002) 1125-1136
[85] T.J. Dolan et al., "Vanadium recycling", Fus. Technol. 26 (1994) 1014-1018
[86] A. Moslang et al., "Suitability and feasibility of the International Fusion Materials Irradiation Facility (IFMIF) for fusion materials studies", Nuclear Fusion 40 (3Y) (2000) 619-627
[87] T. Nakamura et al., "Present status of the fusion neutron source (FNS)", Proc. 4th Symp. on Accelarator Science and Technology, RIKEN, Saitama, 24-26 November (1982) 155-156.
[88] Y. Kasugai et al., "Integral experiment of induced radioactivity in D-T fusion neutron environment and validation of activation cross section library", Fusion Eng. Des. 42 (1998) 299-305
[89] Anil. Kumar et al., "Validation of induced radioactivity calculations for candidate fusion materials through measurements in a graphite-centered assembly", Fusion Eng. Des. 42 (1998) 319-327
[90] C. Konno et al., "Bechmark experiment on bulk shield of SS316/water with simulated superconducting magnet", Fusion Eng. Des. 42 (1998) 267-273
[91] I. Murata et al., "Bechmark experiment on $LiAlO_2$, Li_2TiO_3 and Li_2ZrO_3 assemblies with D-T neutrons-leakage neutron spectrum measurement", Fusion Eng. Des. 51-52 (2000) 821-827
[92] S. Sato et al., "Progress in the blanket neutronics experiment at JAERI/FNS", Fusion Eng. Des. 81 (2006) 1183-1193
[93] Yury Verzilov et al., "The integral experiment on beryllium with D-T

neutrons for verification of tritium breeding", Fusion Eng. Des. 82 (2007) 1-9

[94] A.B. Pashchenko, H. Wienke, IAEA-NDS-176, International Atomic Energy Agency, 1998

ACKNOWLEDGEMENTS

I am very grateful to my supervisor – Prof. Takeo MUROGA of National Institute for Fusion Science (NIFS) in Japan and The Graduate University of Advanced Studies (Sokendai) in Japan, for his aborative guidance, knowledge and kind helps.

I would like to thank Dr. T. Tanaka for his guided advices and powerful helps on this study.

I wish to thank Prof. N. Noda, Prof. A. Nishimura and Prof. A. Sagara of NIFS for their guided comments. Thanks also to other members of Fusion Engineering Research Center (FERC) of NIFS for their kind helps.

I am thankful to Dr. S. Sato for his guidance and collaborations on the irradiation experiments with FNS. I am also thankful to the staff of FNS for their excellent operation of the neutron source at FNS facility.

I also thank the staff of Sokendai in NIFS for their helps. Special thanks should go to Ms. S. Urushihara, Ms. K. Mizuno and Ms. K. Shimazaki. Thanks also to Dr. Yao Zhenyu, Dr. LI Hailin, Mr. XU Qi and Ms. LI Yanfen as classmates of Sokendai for their helps and friendships.

I am also grateful to Prof. Feng Kaiming of SWIP in China for his encouragement during my time in Sokendai.

Finally, I would like to thank my family for their constant love and support.

Li Zaixin
July 29, 2007